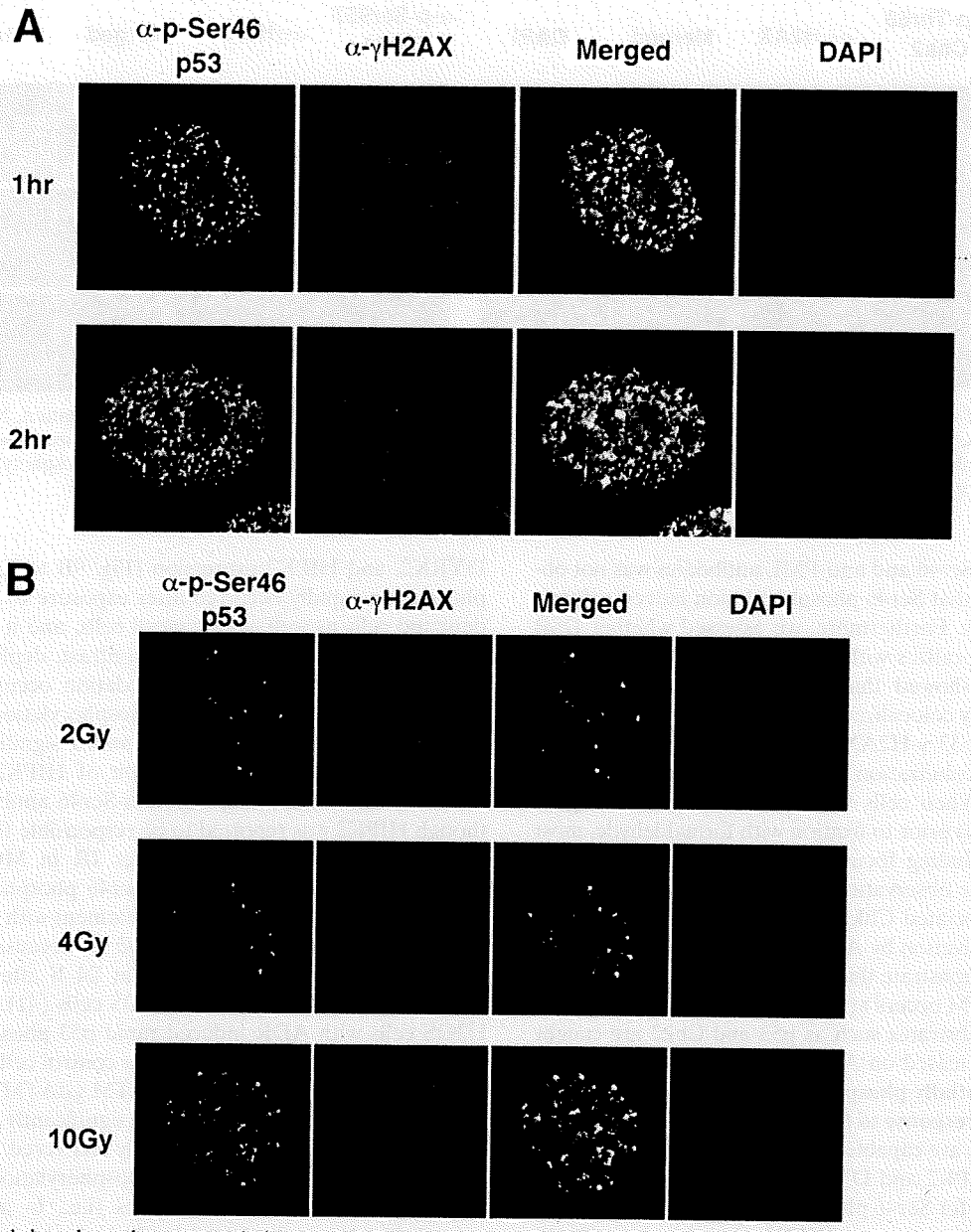

FIG. 7. Dose- and time-dependent accumulation of phospho-Ser46 foci. (A) MCF7 cells were exposed to 0 Gy (−) or 10 Gy (+) of IR and subjected to confocal immunofluorescent analysis at 1 or 2 h after irradiation. Immunofluorescence with anti-phospho-Ser46-of-p53 (green) and anti-γ-H2AX (red) antibodies. DAPI (blue) is also shown. (B) MCF7 cells were exposed to the indicated doses of IR and subjected to confocal immunofluorescent analysis at 30 min after irradiation. Immunofluorescence with anti-phospho-Ser46-of-p53 (green) and anti-γ-H2AX (red) antibodies. DAPI (blue) is also shown. α, anti.

tibody against phospho-Ser46 of p53 showed that Ser46-phosphorylated p53 was observed as foci (Fig. 6B) that partially colocalized with γ-H2AX (Fig. 6D) and Ser1981-phosphorylated ATM (Fig. 6E) but not the PML body (Fig. 6F), which has been known to form another nuclear focus. The foci of fluorescence signals from phospho-Ser46 of p53 in immunofluorescence were confirmed to be p53 itself by RNAi-directed ablation of p53 expression (Fig. 6A and B). Dose dependency of IR and time kinetic experiments showed that foci of phospho-Ser46 gradually increased in a dose-dependent manner and were observed even in cells irradiated at a lower dose (2 Gy, 30 min) (Fig. 7), at which Ser46 phosphorylation was not detected by immunoblot assays. The reason why phospho-Ser46 was not detected in immunoblots may be explained by Ser46-phosphorylated p53 in cells being diluted to perform immunoblot assays, whereas phospho-Ser46 concentrates as foci, subsequently observed by immunofluorescence. We also conducted fluorescence resonance energy transfer (FRET) experiments to show colocalization of phospho-Ser46 with DSB sites. As shown in Fig. 6F, a FRET signal was detected in immunofluorescence with anti-phospho-Ser46 and anti-γ-H2AX antibodies; whereas FRET from immunofluorescence

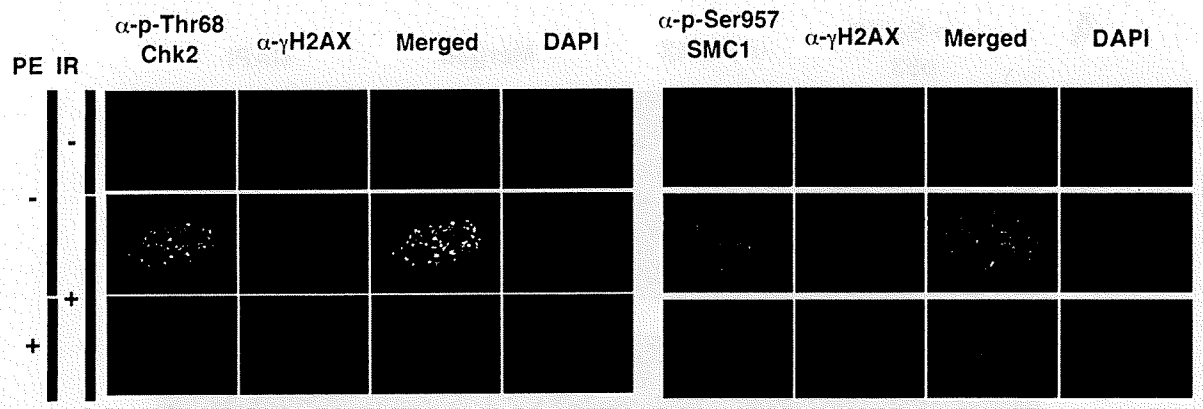

FIG. 8. Release of other ATM substrates from chromatin by preextraction of a detergent prior to formaldehyde fixation. MCF7 cells were exposed to 0 Gy (−) or 10 Gy (+) of IR and subjected to confocal immunofluorescent analysis 30 min after irradiation. To assess whether activated ATM (Ser1981-phosphorylated ATM) or protein phosphorylated by ATM (Thr68-phosphorylated Chk2, Ser957-phosphorylated SMC1, or γ-H2AX) is tightly associated with DSB, preextraction (PE) before fixation was performed. α, anti.

with anti-phospho-Ser46 and anti-PML antibodies was not observed, confirming that Ser46 phosphorylation indeed colocalized with DSB sites. Furthermore, we assessed whether DSB foci (γ-H2AX) colocalizes with Chk2 and SMC1. Immunofluorescent analyses showed that phosphoforms of Chk2 and SMC1 were partially colocalized with DSB foci (Fig. 8), as seen in phospho-Ser46-p53/γ-H2AX (Fig. 6D). We also assessed the effect of permeabilization of cells on the phospho-Ser46 focus formation. When cells were treated with a detergent (0.2% Triton X-100) prior to fixation with formaldehyde, most p53 molecules, including focus-associated p53, were washed out (Fig. 6E). These observations are similar to previous findings that focus-associated Chk2 immediately dissociates from chromatin after activation by ATM-mediated phosphorylation (4). These data demonstrate that Ser46 phosphorylation of p53 by IR-activated ATM occurs at the sites of DSBs, and it seems that some ATM substrates such as p53 and Chk2 are caught and immediately released on ATM-associated foci.

Ser46 is preferentially phosphorylated by ATM in the early inductive phase of response to DNA damage. Although several protein kinases that are capable of phosphorylating Ser46 have been identified, HIPK2 and DYRK2 are the most prominent kinases responsible for Ser46 phosphorylation (6, 9, 33, 41, 49). According to previous reports, HIPK2 phosphorylates Ser46 following exposure to UV (16), but it is controversial whether this kinase actually responds to double-strand breaks because Taira et al. have reported that HIPK2 is a specific kinase serving in a UV-mediated pathway (9, 16, 41). Another Ser46 kinase, DYRK2, phosphorylates following treatment with adriamycin (ADR), a radiomimetic DNA-damaging reagent (41). Although Ser46 phosphorylation observed in this report was obtained at late-phase response to DNA damage, a kinase responsible for Ser46 phosphorylation occurring at early-phase response to IR remains unidentified. Therefore, we next investigated whether ATM is required for Ser46 phosphorylation occurring at early-phase response to IR. In ATM-deficient AT2KY cells, Ser46 was not phosphorylated at early-phase response to DNA damage but became phosphorylated at late phase (Fig. 9A). To define the relation between ATM and other Ser46 kinases, Ser46 phosphorylation was assessed over 24 h under conditions of more than 80% reduction of ATM, DYRK2, and HIPK2 expression (Fig. 9B to E). Ser46 phosphorylation rapidly occurred after exposure to IR in HIPK2-depleted cells as well as in control cells, and it peaked at 2 h after IR treatment (Fig. 9C). In contrast, depletion of ATM causes decreased Ser46 phosphorylation occurring at early-phase response. However, Ser46 phosphorylation was detected after 24 h at a steady-state level and a significant effect on Ser46 phosphorylation by depletion of HIPK2 was not detected by immunoblotting with anti-Ser46 antibody. Thus, although HIPK2 was reported to be responsible for Ser46 phosphorylation observed at 24 h after IR in MCF7 cells (9), HIPK2 knockdown did not alter Ser46 phosphorylation (Fig. 9C). Damage response following treatment with ADR was also assessed using siRNAs (Fig. 9D and E) because DYRK2 was reported to phosphorylate Ser46 at 24 h after exposure to ADR in human osteosarcoma U2OS cells (41). Treatment of U2OS cells with ADR induced rapid p53 phosphorylation at Ser46, and it continued over 24 h in control cells (Fig. 9E). In cells transfected with siRNA for ATM (siATM), Ser46 phosphorylation induced by ADR was significantly attenuated in early phase (Fig. 9E), but it gradually recovered. In contrast, in cells devoid of DYRK2, Ser46 phosphorylation was not affected during early response times (i.e., 6- and 12-h time points), but levels decreased by 24 h as expected (Fig. 9E). Again, HIPK2 knockdown using siRNA did not alter Ser46 phosphorylation and had only a marginal effect on Ser46 phosphorylation (Fig. 9E). On the other hand, upon UV treatment, Ser46 phosphorylation is severely affected by HIPK2 knockdown (Fig. 9F), suggesting that HIPK2 seems to be a kinase directed by UV irradiation, at least under our conditions. These observations suggest that ATM is selectively responsible for Ser46 phosphorylation in early-inductive-phase response to DSBs.

DISCUSSION

Here, we found that Ser46 on p53 is directly phosphorylated by ATM in response to IR. Although ATM preferentially phosphorylates S/T-Q sequences (22, 34), the current experiments revealed that Ser46 is phosphorylated by ATM in a conformation-dependent manner, although this site is an S-P

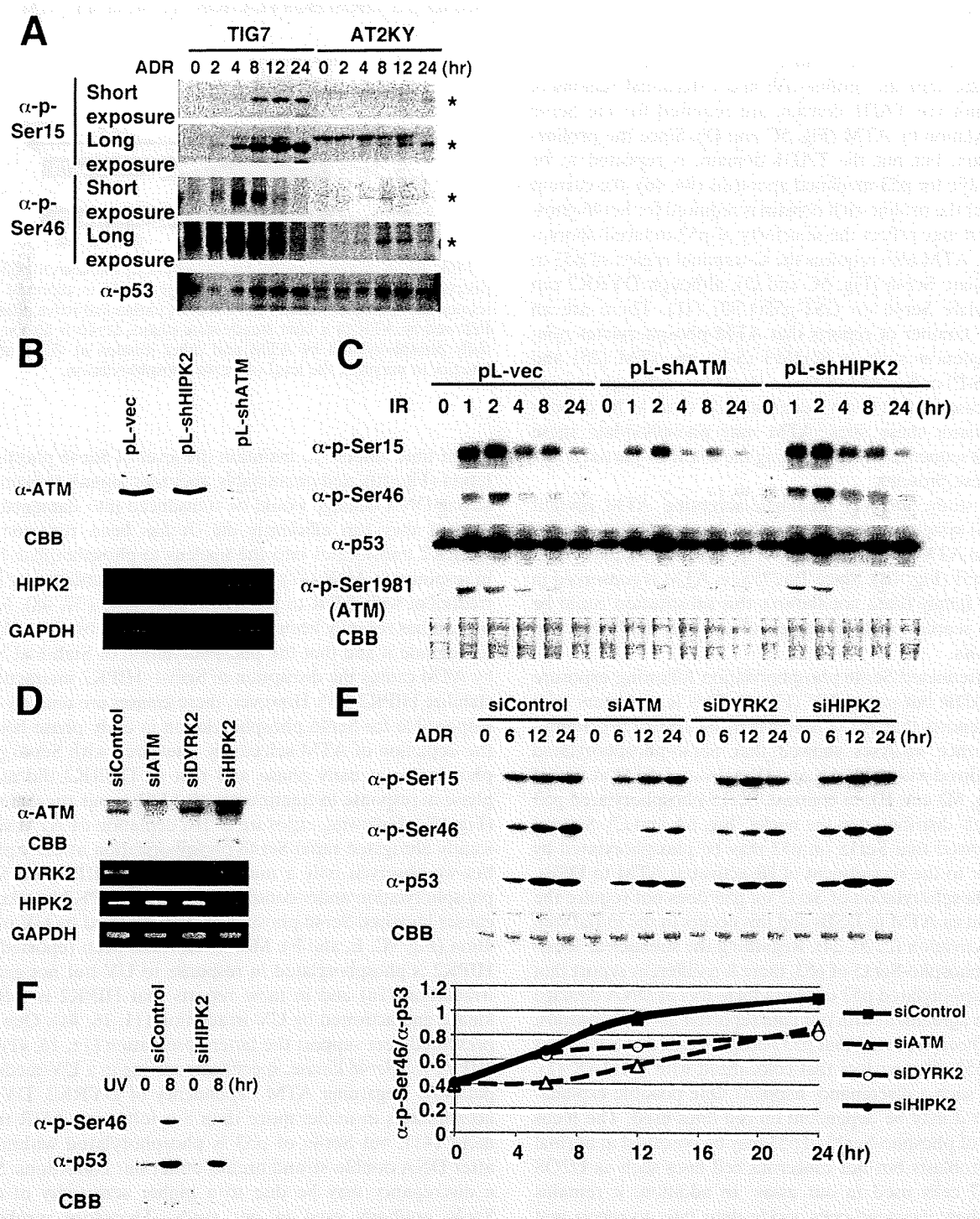

FIG. 9. ATM preferentially phosphorylates p53 at Ser46 in early-phase response to DSBs. (A) Time kinetics of accumulation and phosphorylation of p53 in human fibroblast TIG7 cells or AT2KY cells, human fibroblast cells derived from an A-T patient, treated with 3 μM ADR for indicated periods. Cell lysates were assayed as described for Fig. 1B. Stars indicate bands specific to antibodies. (B and C) ATM is required for Ser46 phosphorylation of p53 in early-phase response to IR. (B) Expression of ATM or HIPK2 in MCF7 cells infected with control lentiviruses (pL-control) or lentiviruses encoding shRNA to HIPK2 (pL-shHIPK2) or ATM (pL-shATM). Expression of ATM was examined by immunoblotting. Expression of HIPK2 was examined by RT-PCR. Coomassie brilliant blue (CBB) staining and RT-PCR of GAPDH are shown for loading controls. (C) Time kinetics of accumulation and phosphorylation of p53 after cellular exposure to IR of 10 Gy. Cell lysates were assayed as described for Fig. 1B. (D to F) ATM is required for Ser46 phosphorylation of p53 in early-phase response to ADR. (D) Expression of ATM, DYRK2, or HIPK2 in U2OS cells transfected with either control siRNA (siControl), siRNA to ATM (siATM), DYRK2 (siDYRK2), or HIPK2 (siHIPK2). The expression level of ATM was determined by immunoblotting, and expression levels of DYRK2 and HIPK2 were determined by RT-PCR. As loading controls, CBB staining and RT-PCR of GAPDH are also indicated. (E and F) Accumulation of p53 and Ser46 phosphorylation occurred in early-phase response to ADR or UV irradiation. U2OS cells transfected with indicated siRNAs were treated with 0.5 μM ADR (E) or 30 J/m^2 UV (F) for indicated periods, and cell lysates were assayed as described in Fig. 1B. The amount of Ser46-phosphorylated p53 was calculated by dividing the value of phosphorylated p53 by that of total p53 at that time point.

sequence (data not shown). Analyses with deletion mutants of p53 revealed that the proline-rich and C-terminal regions of p53, but not the TAD1 domain, are required for the Ser46 phosphorylation by ATM (Fig. 5C and D). Since the proline-rich domain, but not the TAD1 domain, is reported to be indispensable for p53-mediated apoptosis (44, 46), the current finding that the proline-rich domain is required for Ser46 phosphorylation may reflect the selectivity of p53-induced apoptosis. Again, ATM also requires the C-terminal region of p53 to phosphorylate Ser46 (Fig. 5C and D), although DYRK2 can phosphorylate Ser46 on GST-p53(1-92) (41). There are an increasing number of reports that ATM phosphorylates non-S/T-Q sequences such as Ser1893 (S-E) on ATM (25) and Ser1189 (S-P) or Ser1452 (S-G) on Brca1 (8), although in none of these cases has it been demonstrated that ATM directly phosphorylates these sites. ATM may phosphorylate these non-S/T-Q sequences by recognizing the whole or partial structure of these proteins.

In this study, an ATP analogue-accepting ATM mutant (ATM-AS) system was constructed by alanine substitution for Tyr2755 on ATM to confirm that ATM directly phosphorylates Ser46 on p53 (Fig. 4B). Since Tyr2755 on ATM is conserved in the PI3-K family (data not shown), this substitution could be applied to search for direct targets of not only ATM but also other PI3-Ks.

ATM attenuated Ser46 phosphorylation following exposure to IR or ADR but not to UV (Fig. 1). This is consistent with previous reports that ATM is activated by DSBs (19). Immunofluorescence analyses showed that Ser46-phosphorylated p53 colocalized with γ-H2AX and IR-activated ATM at foci of DSBs (Fig. 6D and E); in contrast, Ser15-phosphorylated p53 was diffusely distributed in the nuclei (Fig. 6A and C). Several groups showed that Ser15 on p53 may be phosphorylated by ATM prior to the recruitment of IR-activated ATM to DSBs, because phosphorylation of Ser15 on p53 does not require the recruitment of ATM to DSBs and this occurs in the initial step of ATM activation (2, 20, 24). Regarding the subnuclear localization of phospho-Ser15 of p53, there is a different report that Ser15-phosphorylated p53 does not form foci at DNA damage sites (4), in agreement with our data reported here. In contrast, it has also been reported that p53 phosphorylated at Ser15, but not bulk p53, formed foci that colocalized with γ-H2AX (1). Why does such a discrepancy happen? One possible explanation is that it may be dependent on cell lines used. The focus formation of phospho-Ser15 of p53 may be observed in normal diploid fibroblasts but not cancerous cell lines such as U2OS and MCF7 cells used in our assay. In addition, it remains enigmatic how damaged cells decide their fate: to repair and live or to die. The current observation that Ser46 is phosphorylated by ATM at DSBs may explain the previous report that phosphorylation of Ser15 on p53 is much more sensitive to cell damage and occurs rapidly compared to phosphorylation at Ser46, which is important for induction of apoptosis (33).

Time course experiments revealed that depletion of ATM selectively interfered with Ser46 phosphorylation at early phase (Fig. 9C and E). In response to IR, Ser15 is sequentially phosphorylated by ATM at an earlier inductive phase and by an A-T and Rad3-related (ATR) kinase at a later steady-state phase (Fig. 10) (42). Our data also suggest that Ser46 is sequentially phosphorylated by ATM and other kinases at different time kinetics to maintain the level of Ser46 phosphorylation (Fig. 10), and presumably apoptotic signals triggered by strong DNA damage would be transduced into damaged cells so that they can efficiently die. It has been reported that DYRK2 translocates into the nucleus to phosphorylate Ser46 in response to ADR (41) and that HIPK2 is stabilized by IR or treatment with ADR to phosphorylate Ser46 (37, 48). Moreover, it has recently been reported that Siah-1 binds to HIPK2 to degrade it and that the phosphorylation of Siah-1 at Ser19 by ATM causes the disruption of Siah-1–HIPK2 interaction to stabilize HIPK2 (48). However, these kinases are unlikely to be responsible for Ser46 phosphorylation in early phase because the depletion of ATM selectively interfered with Ser46 phosphorylation at early phase and that of DYRK2 did at late phase in response to treatment with ADR in our present study (Fig. 9E). Following exposure to IR, depletion of ATM significantly abrogated rapid Ser46 phosphorylation at early phase, but we observed only a marginal effect of HIPK2 on Ser46 phosphorylation under conditions in which HIPK2 knockdown causes impaired Ser46 phosphorylation directed by UV irradiation (Fig. 9C, E, and F). Moreover, it has been reported that HIPK2 is phosphorylated in response to UV but not gamma irradiation (16) and in most reports that HIPK2 is a Ser46 kinase and activated by UV irradiation (11, 16, 41). Our data presented here support the latter observation (11, 16, 41) that HIPK2 is a Ser46 kinase, specifically serving in a UV-mediated pathway. Regarding ATM dependency of DYRK2, DYRK2 accumulates in nuclei more than 8 h following ADR treatment (41), but Ser46 of p53 is phosphorylated within 6 h after DNA double-strand breaks under our conditions. Such a discrepancy may be due to a higher sensitivity of anti-Ser46 antibody used in our study. Therefore, probably, DYRK2 seems to be dependent on ATM and may be required for Ser46 phosphorylation occurring at late-phase response of DNA double-strand breaks.

In our present study, IR-activated ATM is partially colocalized with Ser46-phosphorylated p53 in response to DNA damage, suggesting that p53 phosphorylation at Ser46 is required to trigger early apoptotic signals to damaged cells. The reason why Ser46-phosphorylated p53 is recruited to DSB sites is still unclear. It has been reported that Chk2 is phosphorylated by ATM near DSB sites and that activated Chk2 releases from DSB sites to function during G_1 and G_2 checkpoints (30, 32). Similarly, activated ATM phosphorylates p53 at Ser46 near

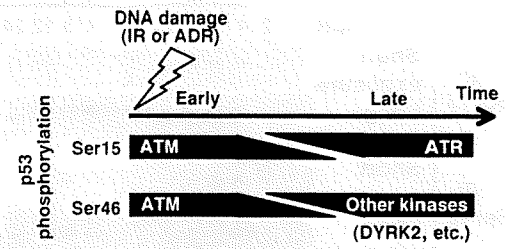

FIG. 10. A proposed model for contribution of kinases to p53 phosphorylation. In response to DNA damage, Ser15 is reported to be sequentially phosphorylated by ATM at an earlier inductive phase and followed by ATR at a later steady-state phase. Ser46 is also sequentially phosphorylated by ATM and other kinases at different time kinetics to maintain the level of Ser46 phosphorylation.

DSB sites and Ser46-phosphorylated p53 may release from DSB sites to promote transcription of proapoptotic genes. Under various stresses, including UV and IR, DYRK2 and HIPK2 may work together with ATM to phosphorylate p53 at Ser46, leading to apoptosis to ensure that severely damaged cells are completely killed, though further investigations are needed to elucidate the molecular mechanisms of ATM-triggered p53-mediated apoptosis.

In conclusion, our present study strongly supports the idea that ATM directly phosphorylates p53 at Ser46 and is required for Ser46 phosphorylation occurring in early-phase DNA damage response. The direct link of ATM to Ser46 phosphorylation of p53 provides new insights into ATM-mediated p53-dependent apoptosis, though it cannot be ruled out that ATM may require adaptor proteins for Ser46 phosphorylation near DSB sites to facilitate its phosphorylation. Here, we show that ATM is likely to directly phosphorylate Ser46 of p53, but the kinase activity for Ser46 may be dependent on unidentified posttranslational modifications of ATM in response to severe DNA damage. In addition, it is quite difficult to determine *bona fide in vivo* kinases responsible for Ser46, so we cannot exclude the possibility that ATM is indirectly involved in the phosphorylation of Ser 46. Therefore, further studies are required to clarify whether ATM is a *bona fide in vivo* kinase responsible for Ser46 phosphorylation.

ACKNOWLEDGMENTS

We are grateful to Michael B. Kastan (St. Jude Children's Research Hospital) for the expression vector for FLAG-tagged ATM wild type. We also thank Kiyotsugu Yoshida (Tokyo Medical and Dental University, Japan) for valuable discussions with respect to DYRK2 and Kyoko Fujinaka (National Cancer Center Research Institute, Japan) for technical assistance.

This work was supported by a Grant-in-Aid for Scientific Research on Priority Areas (17013088) (to Y.T. and M.E.); SORST, Japan Science and Technology (to Y.T.); and a grant from the Takeda Science Foundation (to M.E.).

REFERENCES

1. **Al Rashid, S. T., G. Dellaire, A. Cuddihy, F. Jalali, M. Vaid, C. Coackley, M. Folkard, Y. Xu, B. P. Chen, D. J. Chen, L. Lilge, K. M. Prise, D. P. Bazett Jones, and R. G. Bristow.** 2005. Evidence for the direct binding of phosphorylated p53 to sites of DNA breaks in vivo. Cancer Res. **65**:10810–10821.
2. **Bakkenist, C. J., and M. B. Kastan.** 2003. DNA damage activates ATM through intermolecular autophosphorylation and dimer dissociation. Nature **421**:499–506.
3. **Banin, S., L. Moyal, S. Shieh, Y. Taya, C. W. Anderson, L. Chessa, N. I. Smorodinsky, C. Prives, Y. Reiss, Y. Shiloh, and Y. Ziv.** 1998. Enhanced phosphorylation of p53 by ATM in response to DNA damage. Science **281**:1674–1677.
4. **Bekker-Jensen, S., C. Lukas, R. Kitagawa, F. Melander, M. B. Kastan, J. Bartek, and J. Lukas.** 2006. Spatial organization of the mammalian genome surveillance machinery in response to DNA strand breaks. J. Cell Biol. **173**:195–206.
5. **Bourdon, J. C., V. D. Laurenzi, G. Melino, and D. Lane.** 2003. p53: 25 years of research and more questions to answer. Cell Death Differ. **10**:397–399.
6. **Bulavin, D. V., S. Saito, M. C. Hollander, K. Sakaguchi, C. W. Anderson, E. Appella, and A. J. J. Fornace.** 1999. Phosphorylation of human p53 by p38 kinase coordinates N-terminal phosphorylation and apoptosis in response to UV radiation. EMBO J. **18**:6845–6854.
7. **Canman, C. E., D. S. Lim, K. A. Cimprich, Y. Taya, K. Tamai, K. Sakaguchi, E. Appella, M. B. Kastan, and J. D. Siliciano.** 1998. Activation of the ATM kinase by ionizing radiation and phosphorylation of p53. Science **281**:1677–1679.
8. **Cortez, D., Y. Wang, J. Qin, and S. J. Elledge.** 1999. Requirement of ATM-dependent phosphorylation of brca1 in the DNA damage response to double-strand breaks. Science **286**:1162–1166.
9. **Dauth, I., J. Kruger, and T. G. Hofmann.** 2007. Homeodomain-interacting protein kinase 2 is the ionizing radiation-activated p53 serine 46 kinase and is regulated by ATM. Cancer Res. **67**:2274–2279.
10. **Di Stefano, V., C. Rinaldo, A. Sacchi, S. Soddu, and G. D'Orazi.** 2004. Homeodomain-interacting protein kinase-2 activity and p53 phosphorylation are critical events for cisplatin-mediated apoptosis. Exp. Cell Res. **293**:311–320.
11. **D'Orazi, G., B. Cecchinelli, T. Bruno, I. Manni, Y. Higashimoto, S. Saito, M. Gostissa, S. Coen, A. Marchetti, G. Del Sal, G. Piaggio, M. Fanciulli, E. Appella, and S. Soddu.** 2002. Homeodomain-interacting protein kinase-2 phosphorylates p53 at Ser 46 and mediates apoptosis. Nat. Cell Biol. **4**:11–19.
12. **Endo, Y., A. Sugiyama, S. A. Li, K. Ohmori, H. Ohata, Y. Yoshida, M. Shibuya, K. Takei, M. Enari, and Y. Taya.** 2008. Regulation of clathrin-mediated endocytosis by p53. Genes Cells **13**:375–386.
13. **Giaccia, A. J., and M. B. Kastan.** 1998. The complexity of p53 modulation: emerging patterns from divergent signals. Genes Dev. **12**:2973–2983.
14. **Habelhah, H., K. Shah, L. Huang, A. L. Burlingame, K. M. Shokat, and Z. Ronai.** 2001. Identification of new JNK substrate using ATP pocket mutant JNK and a corresponding ATP analogue. J. Biol. Chem. **276**:18090–18095.
15. **Harris, S. L., and A. J. Levine.** 2005. The p53 pathway: positive and negative feedback loops. Oncogene **24**:2899–2908.
16. **Hofmann, T. G., A. Moller, H. Sirma, H. Zentgraf, Y. Taya, W. Droge, H. Will, and M. L. Schmitz.** 2002. Regulation of p53 activity by its interaction with homeodomain-interacting protein kinase-2. Nat. Cell Biol. **4**:1–10.
17. **Hofmann, T. G., N. Stollberg, M. L. Schmitz, and H. Will.** 2003. HIPK2 regulates transforming growth factor-beta-induced c-Jun NH(2)-terminal kinase activation and apoptosis in human hepatoma cells. Cancer Res. **63**:8271–8277.
18. **Ichwan, S. J., S. Yamada, P. Sumrejkanchanakij, E. Ibrahim-Auerkari, K. Eto, and M. A. Ikeda.** 2006. Defect in serine 46 phosphorylation of p53 contributes to acquisition of p53 resistance in oral squamous cell carcinoma cells. Oncogene **25**:1216–1224.
19. **Ismail, I. H., S. Nyström, J. Nygren, and O. Hammarsten.** 2005. Activation of ataxia telangiectasia mutated by DNA strand break-inducing agents correlates closely with the number of DNA double strand breaks. J. Biol. Chem. **280**:4649–4655.
20. **Kanu, N., and A. Behrens.** 2007. ATMIN defines an NBS1-independent pathway of ATM signalling. EMBO J. **26**:2933–2941.
21. **Khanna, K. K., K. E. Keating, S. Kozlov, S. Scott, M. Gatei, K. Hobson, Y. Taya, B. Gabrielli, D. Chan, S. P. Lees-Miller, and M. F. Lavin.** 1998. ATM associates with and phosphorylates p53: mapping the region of interaction. Nat. Genet. **20**:398–400.
22. **Kim, S. T., D. S. Lim, C. E. Canman, and M. B. Kastan.** 1999. Substrate specificities and identification of putative substrates of ATM kinase family members. J. Biol. Chem. **274**:37538–37543.
23. **Kinoshita, A., H. Fukumoto, T. Shah, C. M. Whelan, M. C. Irizarry, and B. T. Hyman.** 2003. Demonstration by FRET of BACE interaction with the amyloid precursor protein at the cell surface and in early endosomes. J. Cell Sci. **116**:3339–3346.
24. **Kitagawa, R., C. J. Bakkenist, P. J. McKinnon, and M. B. Kastan.** 2004. Phosphorylation of SMC1 is a critical downstream event in the ATM-NBS1-BRCA1 pathway. Genes Dev. **18**:1423–1438.
25. **Kozlov, S. V., M. E. Graham, C. Peng, P. Chen, P. J. Robinson, and M. F. Lavin.** 2006. Involvement of novel autophosphorylation sites in ATM activation. EMBO J. **25**:3504–3514.
26. **Lavin, M. F., and Y. Shiloh.** 1997. The genetic defect in ataxia-telangiectasia. Annu. Rev. Immunol. **15**:177–202.
27. **Li, X., P. Dumont, A. Della Pietra, C. Shetler, and M. E. Murphy.** 2005. The codon 47 polymorphism in p53 is functionally significant. J. Biol. Chem. **280**:24245–24251.
28. **Lu, H., Y. Taya, M. Ikeda, and A. J. Levine.** 1998. Ultraviolet radiation, but not gamma radiation or etoposide-induced DNA damage, results in the phosphorylation of the murine p53 protein at serine-389. Proc. Natl. Acad. Sci. U. S. A. **95**:6399–6402.
29. **Matsuoka, S., B. A. Ballif, A. Smogorzewska, E. R. McDonald III, K. E. Hurov, J. Luo, C. E. Bakalarski, Z. Zhao, N. Solimini, Y. Lerenthal, Y. Shiloh, S. P. Gygi, and S. J. Elledge.** 2007. ATM and ATR substrate analysis reveals extensive protein networks responsive to DNA damage. Science **316**:1160–1166.
30. **Matsuoka, S., G. Rotman, A. Ogawa, Y. Shiloh, K. Tamai, and S. J. Elledge.** 2000. Ataxia telangiectasia-mutated phosphorylates Chk2 in vivo and in vitro. Proc. Natl. Acad. Sci. U. S. A. **97**:10389–10394.
31. **Meek, D. W., and C. W. Anderson.** 2009. Posttranslational modification of p53: cooperative integrators of function. Cold Spring Harbor Perspect. Biol. **1**:a000950.
32. **Melchionna, R., X. B. Chen, A. Blasina, and C. H. McGowan.** 2000. Threonine 68 is required for radiation-induced phosphorylation and activation of Cds1. Nat. Cell Biol. **2**:762–765.
33. **Oda, K., H. Arakawa, T. Tanaka, K. Matsuda, C. Tanikawa, T. Mori, H. Nishimori, K. Tamai, T. Tokino, Y. Nakamura, and Y. Taya.** 2000. p53AIP1, a potential mediator of p53-dependent apoptosis, and its regulation by Ser-46-phosphorylated p53. Cell **102**:849–862.
34. **O'Neill, T., A. J. Dwyer, Y. Ziv, D. W. Chan, S. P. Lees-Miller, R. H. Abraham, J. H. Lai, D. Hill, Y. Shiloh, L. C. Cantley, and G. A. Rathbun.**

2000. Utilization of oriented peptide libraries to identify substrate motifs selected by ATM. J. Biol. Chem. **275**:22719–22727.
35. **Oren, M.** 2003. Decision making by p53: life, death and cancer. Cell Death Differ. **10**:431–442.
36. **Prives, C.** 1998. Signaling to p53: breaking the MDM2-p53 circuit. Cell **95**:5–8.
37. **Rinaldo, C., A. Prodosmo, F. Mancini, S. Iacovelli, A. Sacchi, F. Moretti, and S. Soddu.** 2007. MDM2-regulated degradation of HIPK2 prevents p53Ser46 phosphorylation and DNA damage-induced apoptosis. Mol. Cell **25**:739–750.
38. **Saito, S., A. A. Goodarzi, Y. Higashimoto, Y. Noda, S. P. Lees-Miller, E. Appella, and C. W. Anderson.** 2002. ATM mediates phosphorylation at multiple p53 sites, including Ser(46), in response to ionizing radiation. J. Biol. Chem. **277**:12491–12494.
39. **Shah, K., Y. Liu, C. Deirmengian, and K. M. Shokat.** 1997. Engineering unnatural nucleotide specificity for Rous sarcoma virus tyrosine kinase to uniquely label its direct substrates. Proc. Natl. Acad. Sci. U. S. A. **94**:3565–3570.
40. **Shieh, S. Y., M. Ikeda, Y. Taya, and C. Prives.** 1997. DNA damage-induced phosphorylation of p53 alleviates inhibition by MDM2. Cell **91**:325–334.
41. **Taira, N., K. Nihira, T. Yamaguchi, Y. Miki, and K. Yoshida.** 2007. DYRK2 is targeted to the nucleus and controls p53 via Ser46 phosphorylation in the apoptotic response to DNA damage. Mol. Cell **25**:725–738.
42. **Tibbetts, R. S., K. M. Brumbaugh, J. M. Williams, J. N. Sarkaria, W. A. Cliby, S. Y. Shieh, Y. Taya, C. Prives, and R. T. Abraham.** 1999. A role for ATR in the DNA damage-induced phosphorylation of p53. Genes Dev. **13**:152–157.
43. **Ubersax, J. A., E. L. Woodbury, P. N. Quang, M. Paraz, J. D. Blethrow, K. Shah, K. M. Shokat, and D. O. Morgan.** 2003. Targets of the cyclin-dependent kinase Cdk1. Nature **425**:859–864.
44. **Venot, C., M. Maratrat, C. Dureuil, E. Conseiller, L. Bracco, and L. Debussche.** 1998. The requirement for the p53 proline-rich functional domain for mediation of apoptosis is correlated with specific PIG3 gene transactivation and with transcriptional repression. EMBO J. **17**:4668–4679.
45. **Walker, E. H., M. E. Pacold, O. Perisic, L. Stephens, P. T. Hawkins, M. P. Wymann, and R. L. Williams.** 2000. Structural determinants of phosphoinositide 3-kinase inhibition by wortmannin, LY294002, quercetin, myricetin, and staurosporine. Mol. Cell **6**:909–919.
46. **Walker, K. K., and A. J. Levine.** 1996. Identification of a novel p53 functional domain that is necessary for efficient growth suppression. Proc. Natl. Acad. Sci. U. S. A. **93**:15335–15340.
47. **Ward, I. M., X. Wu, and J. Chen.** 2001. Threonine 68 of Chk2 is phosphorylated at sites of DNA strand breaks. J. Biol. Chem. **276**:47555–47558.
48. **Winter, M., D. Sombroek, I. Dauth, J. Moehlenbrink, K. Scheuermann, J. Crone, and T. G. Hofmann.** 2008. Control of HIPK2 stability by ubiquitin ligase Siah-1 and checkpoint kinases ATM and ATR. Nat. Cell Biol. **10**:812–824.
49. **Yoshida, K., H. Liu, and Y. Miki.** 2006. Protein kinase C delta regulates Ser46 phosphorylation of p53 tumor suppressor in the apoptotic response to DNA damage. J. Biol. Chem. **281**:5734–5740.

doi:10.1016/j.jmb.2009.09.029 J. Mol. Biol. (2009) 394, 460–471

JMB

Available online at www.sciencedirect.com

ScienceDirect

ELSEVIER

Identification of a Function-Specific Mutation of Clathrin Heavy Chain (CHC) Required for p53 Transactivation

Hirokazu Ohata[1,2], Nobuyuki Ota[3], Mikako Shirouzu[4], Shigeyuki Yokoyama[4,5], Jun Yokota[2], Yoichi Taya[6]* and Masato Enari[1,2]*

[1]*Radiobiology Division, National Cancer Center Research Institute, Tsukiji 5-1-1, Chuo-ku, Tokyo 104-0045, Japan*

[2]*Biology Division, National Cancer Center Research Institute, Tsukiji 5-1-1, Chuo-ku, Tokyo 104-0045, Japan*

[3]*A-Cube Inc. and Musashino University, Research Institute of Pharmaceutical Sciences, Tokyo, Japan*

[4]*Systems and Structural Biology Center, RIKEN Yokohama Institute, 1-7-22 Suehiro-cho, Tsurumi, Yokohama 230-0045, Japan*

[5]*Department of Biophysics and Biochemistry, Graduate School of Science, The University of Tokyo, 7-3-1 Hongo, Bunkyo-ku, Tokyo 113-0033, Japan*

[6]*Cancer Science Institute of Singapore, National University of Singapore, Center for Life Sciences, #02-07, 28 Medical Drive, Singapore 117456*

Received 19 June 2009; received in revised form 14 September 2009; accepted 14 September 2009
Available online 18 September 2009

Edited by P. Wright

The p53 pathway is activated in response to various cellular stresses to protect cells from malignant transformation. We have previously shown that clathrin heavy chain (CHC), which is a cytosolic protein regulating endocytosis, is present in nuclei and binds to p53 to promote p53-mediated transcription. However, details of the binding interface between p53 and CHC remain unclear. Here, we report on the binding mode between p53 and CHC using mutation analyses and a structural model of the interaction generated by molecular dynamics. Structural modeling analyses predict that an Asn1288 residue in CHC is crucial for binding to p53. In fact, substitution of this Asn to Ala of CHC diminished its ability to interact with p53, leading to reduced activity to transactivate p53. Surprisingly, this mutation had little effect on receptor-mediated endocytosis. Thus, the function-specific mutation of CHC will clarify physiological roles of CHC in the regulation of the p53 pathway.

Keywords: clathrin heavy chain; p53; structural modeling; transcription; tumor suppressor

*Corresponding authors. E-mail addresses: csiyt@nus.edu.sg; menari@ncc.go.jp.

Abbreviations used: ActD, actinomycin D; BSA, bovine serum albumin; CHC, clathrin heavy chain; CLC, clathrin light chain; DMEM, Dulbecco's modified Eagle's medium; GST, glutathione S-transferase; HRP, horseradish peroxidase; MCSA-PCR, multi-conformation simulated annealing pseudo-crystallographic refinement; PARP, poly-ADP ribose polymerase; RT-PCR, reverse transcriptase–polymerase chain reaction; UTR, untranslated region.

Introduction

The tumor suppressor p53 protein is a transcription factor that protects cells from malignant transformation. The p53 pathway is activated in response to various cellular stresses such as DNA damage, oncogene activation, and hypoxia. Upon activation, p53 exerts its tumor suppressor activity by inducing cell-cycle arrest, apoptosis, or senescence.[1–7] Because mutations in the p53 gene have been found in around 50% of human cancers and most mutations of p53 in tumors are located in the central DNA-binding domain, transcriptional regulation by p53 is thought to be most important for prevention of tumorigenesis.[8] Thus, analysis of p53-mediated transcriptional mechanisms is indispensable for elucidation of tumorigenesis and development of new antitumor drugs. Although many factors that contribute to the regulation of p53 activity have been reported,[1,5,6,9] detailed mechanisms remain to be elucidated.

We have previously reported that clathrin heavy chain (CHC), which is a cytosolic protein involved in receptor-mediated endocytosis and intracellular trafficking and recycling of receptors,[10–12] is present in nuclei and enhances p53-mediated transcription.[13] The presence of CHC in nuclei and nuclear matrices was confirmed by other groups.[13–15] We have also shown that p53 interacts with CHC not only in nuclei but also in cytosol and regulates clathrin-mediated endocytosis through the association with CHC.[16]

In the clathrin-mediated endocytic pathway, clathrin is composed of a trimer of CHC and is associated with each clathrin light chain (CLC), called triskelion, and they further assemble to form a polyhedral cage-like structure.[17] Polyhedral clathrin is recruited to the plasma membrane and promotes the internalization and recycling of receptors participating in signal transduction events.[18] CHC consists of an N-terminal β-propeller domain that is necessary for binding to adaptor proteins for the internalization of various molecules, followed by seven α-helical repeat structures named 'clathrin repeats'.[17] In addition, it has been reported that CHC plays a role in mitosis.[19] In the C-terminus, CHC possesses a trimerization domain essential for stable formation of the polyhedral clathrin structure and CLC-binding domain.[20] We have recently reported that CHC bearing residues from 833 to 1406 (CHC833–1406) lacking trimerization and CLC-binding domains interact with p53 and enhance p53 transactivation.[21] Thus, the oligomerization of CHC, which is critical for endocytosis and mitosis,[20,22,23] has not been necessary for p53-mediated transcription, supporting our proposition that CHC has an alternative function as a co-activator for p53 and an additional role in the regulation of endocytosis and mitosis.[21] However, although our findings support that CHC functions as a co-activator of p53, there is a limitation to investigate the physiological roles of CHC in the p53-mediated pathway because CHC ablation in examining the impact on p53 transactivation may cause some effects on vesicle transport and endocytosis. Therefore, the exploration of function-specific mutations of CHC for the p53 pathway is important for elucidation of mechanisms by which CHC transactivates p53.

We have previously found that there is a considerable similarity between p53 and CLC in the CHC-binding region.[13] However, the detailed binding interface between p53 and CHC remains to be determined. Thus, the construction of a structural model of the p53–CHC interface provides further insights into regulation of p53 transactivation by CHC. In this study, we show that conserved hydrophobic residues between p53 and CLC are important for p53 transactivation and that p53 function correlates positively with the interaction with CHC. Moreover, *in silico* structural prediction of the interface between p53 and CHC reveals that the Asn1288 residue in CHC is essential for binding to p53. Interestingly, the substitution of this Asn to Ala (CHC-N1288A) diminishes its ability to transactivate p53 without any effect on receptor-mediated endocytic activity.

Results

Conserved residues between p53 and CLC are required for the interaction with CHC to enhance p53 transactivation

We have previously reported that the N-terminal region of p53 is required for binding to CHC using various deletion mutants of p53.[13,21] In our previous report, we noticed a significant similarity of the N-terminal transactivation domain of p53 to the CHC-binding region of CLC and that various hydrophobic residues are conserved in human p53 (Fig. 1a).[13] To assess whether these conserved residues are required for the interaction with CHC, we generated four p53 point mutants (L43A, I50A, L43A/I50A, and W53R) as glutathione *S*-transferase (GST) fusion proteins and carried out an *in vitro* binding assay using ^{35}S-labeled CHC as described previously.[13] A GST pull-down assay showed that the CHC-binding affinity of all p53 proteins bearing mutations in conserved residues is lower than that of wild-type p53 (Fig. 1b). Furthermore, we assessed the effect of p53 mutations on the binding to endogenous CHC in cells. FLAG-tagged p53 proteins were expressed in p53-null cells, and cell lysates were immunoprecipitated with anti-FLAG antibody followed by immunoblotting with indicated antibodies. Immunoprecipitation assay shows that these mutations cause reduced interaction with CHC (Fig. 1c).

To examine the effect of these p53 mutants on p53 transactivation, we performed reporter assays using promoters of p53-target genes. Reporter assays using various p53 mutants show that mutations of p53 at N-terminal conserved residues cause marked reduction of transactivation of p53-target genes such as p53AIP1 (Fig. 2a) and p21 (Fig. 2b). To confirm

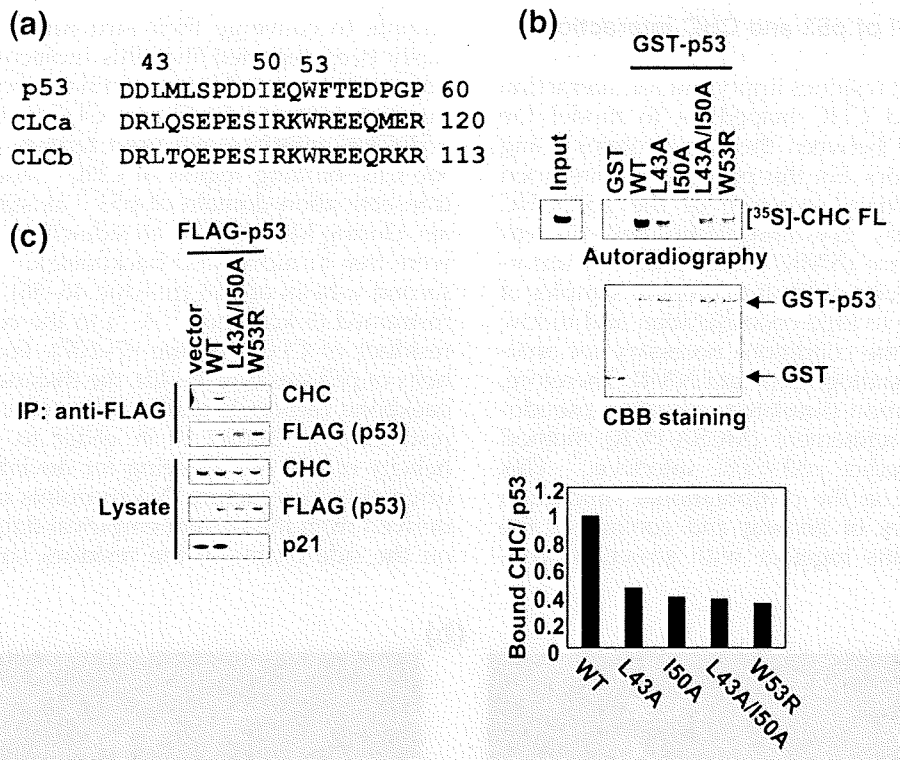

Fig. 1. Conserved residues in p53 are required for the interaction with CHC. (a) Alignments of the CHC-binding region of human p53, CLCa, and CLCb. (b and c) Conserved residues in p53 are required for interaction with CHC. (b) ^{35}S-labeled full-length CHC was synthesized by an *in vitro* transcription-coupled translation system using rabbit reticulocyte lysates. Lysates containing ^{35}S-labeled CHC were mixed with GST or GST-p53 derivatives immobilized on glutathione-Sepharose 4B beads for binding assay (upper panel). GST and GST-p53 proteins used for binding assay were stained by CBB (middle panel). The graph represents the ratio of bound CHC to GST or GST-p53, as quantified by Image J densitometry (lower panel). (c) H1299 cells were transfected with each FLAG-p53 construct. FLAG-p53 proteins in cell lysates were immunoprecipitated by anti-FLAG M2 agarose, and eluates were separated by SDS-PAGE, followed by immunoblotting with indicated antibodies.

the effect of substitutions of these conserved residues on p53 transactivation, we examined the induction of endogenous p53-target genes by immunoblotting. Although the expression level of mutated p53 proteins was the same as that of wild-type p53, the induction of p53-responsive genes such as p21 and Mdm2 by ectopic expression of mutated p53 proteins was strikingly reduced compared with that of wild-type p53 (Fig. 2c). These results suggest that the ability of p53 to bind to CHC correlates with p53 transactivation and indicates that conserved hydrophobic residues between p53 and CLC are important for the transcriptional activity of p53 as well as binding to CHC.

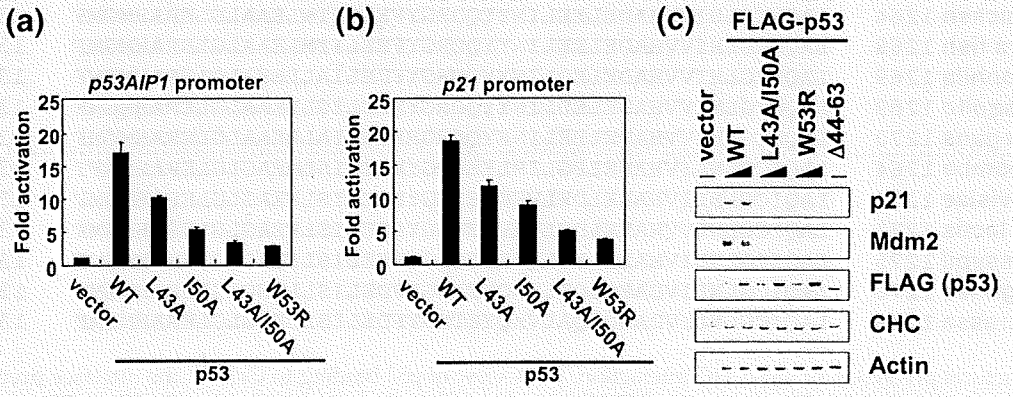

Fig. 2. p53 transactivation correlates with the ability of p53 to bind CHC. (a and b) Conserved residues in p53 are required for p53 transactivation. H1299 cells were transfected with each p53 construct and the p53AIP1 reporter plasmid (a) or p21 reporter plasmid (b), and luciferase activity was measured 24 h after transfection. (c) H1299 cells were transfected with each p53 construct, and whole-cell lysates were analyzed by immunoblotting using the indicated antibodies. Actin was used as a loading control.

Structural model of p53 and CHC interaction

Identification of residues important for interaction between p53 and CHC helped us to model the binding interface between the two proteins using molecular dynamics. For this purpose, we first tried to determine tertiary structure of the p53–CHC complex by X-ray crystallography and nuclear magnetic resonance (NMR) techniques, but unfortunately, it was quite difficult to prepare samples of this complex due to little crystallization and to low solubility under the conditions necessary for analysis by X-ray crystallography and NMR. Therefore, a multi-conformation simulated annealing pseudo-crystallographic refinement (MCSA-PCR) method was used to predict p53–CHC interface.[24] This method is based on the computational simulation of repeated cycles of heating and cooling of the interacting proteins together with structural constraints to converge their structures. It has previously been reported that this molecular dynamics approach was used for preliminary modeling of the interface between CHC and CLC.[25] To model the p53–CHC interface, we used tertiary structures of the CLC-binding region of CHC[25] and N-terminal transactivation domain of p53[26] as starting materials. During MCSA-PCR, all side-chain atoms of p53 were free to move, and backbone C^{α} atoms in the second α-helix of p53 (residue 46–56) were weakly restrained (5 kcal mol^{-1} $Å^{-2}$) to the corresponding residues of CLC (residue 97–107). For the first α-helix of p53 (residue 35–40), the distances of the p53 backbone carbonyls and amides were also weakly restrained to 2.86±1 Å in order to promote the helicity of p53 but allowing for deviation from the original helix structure. No restraints or constraints derived from the current empirical data are applied on the side chains of the residues studied in this

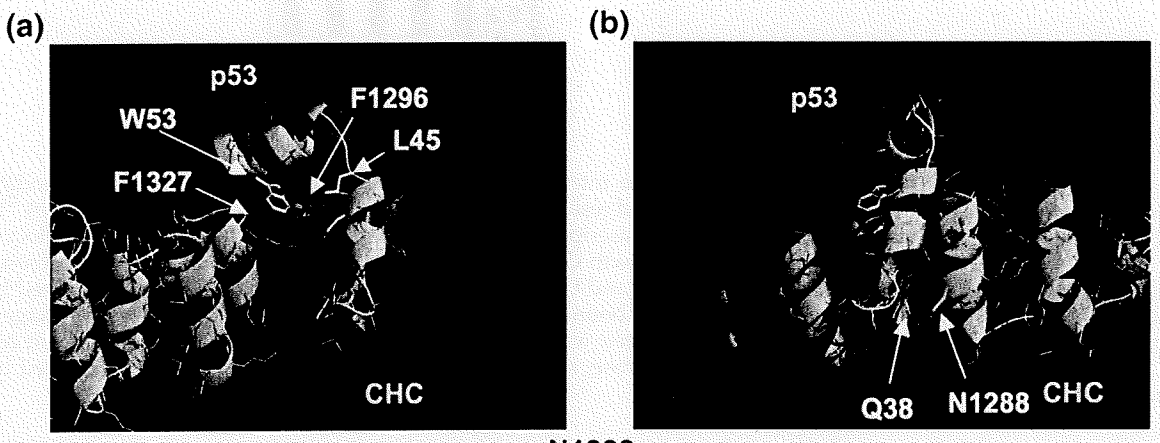

(c)

N1288 ↓

Human 1268	LAQMCGLHIVVHADELEELINYYQDRGYFEELITMLEAALGLERAHMGMF	1317
Chimpanzee 1268	LAQMCGLHIVVHADELEELINYYQDRGYFEELITMLEAALGLERAHMGMF	1317
Dog 1281	LAQMCGLHIVVHADELEELINYYQDRGYFEELITMLEAALGLERAHMGMF	1330
Cattle 1268	LAQMCGLHIVVHADELEELINYYQDRGYFEELITMLEAALGLERAHMGMF	1317
Mouse 1268	LAQMCGLHIVVHADELEELINYYQDRGYFEELITMLEAALGLERAHMGMF	1317
Rat 1268	LAQMCGLHIVVHADELEELINYYQDRGYFEELITMLEAALGLERAHMGMF	1317
Chicken 1264	LAQMCGLHIVVHADELEELINYYQDRGYFEELITMLEAALGLERAHMGMF	1313
Zebra fish 1268	LAQMCGLHIVVHADELEELINYYQDRGYFEELITMLEAALGLERAHMGMF	1317
Drosophila 1269	LAQMCGLHIVVHADELEDLINYYQNRGYFDELIALLESALGLERAHMGMF	1318
Mosquito 1269	LAQMCGLHIVVHADELEDLINYYQDRGYFEELIGLLEAALGLERAHMGMF	1318
C. elegans 1270	LAQMCGLHIVVHADELEELINFYQDRGHFEELIALLEAALGLERAHMGMF	1319
S. pombe 1264	LAQICGLNLIVHAEELPGLIRLYEERGYFEEVISLMEAGLGLERAHMAFY	1313
S. cerevisiae 1274	LAQICGLNLIVHAEELDELVERYESNGYFEELISLFEAGLGLERAHMGMF	1323
K. lactis 1273	LAQICGLNLVVHAEELDELVAVYEHNGYFEELISLFEAGLGLERAHMGMF	1322
E. gossypii 1275	LAQICGLNLIVHAEELKELVDKYESNGYFEELISLFEAGLGLERAHMGMF	1324
M. grisea 1276	LAQICGLNLIVDAEQLQTLVKQYERNGFFDELISLLENGLGLERAHMGMF	1325
N. crassa 1276	LAQICGLNLIVDAEQLQALVKQYETNGYFDELISLLEQGLGLERAHMGMF	1325

Fig. 3. Structural prediction of p53–CHC interaction. (a) A view of p53 binding to CHC at the interface predicted by molecular dynamic simulation. p53 is in cyan and CHC is in green. The aromatic side chain of Trp53 of p53 mediates the interaction with an aromatic side chain of Phe1327 in the hydrophobic cleft of CHC. The side chain of Leu45 of p53 interacts with the aromatic side chain of Phe1296 of CHC through hydrophobic interaction. (b) Structural modeling revealed that the side chain of Asn1288 of CHC is close to the side chain of Gln38 of p53. (c) Asn1288 in CHC is conserved in multicellular organisms from mammals to flies, but this amino acid residue is not present in unicellular organisms such as yeasts and fungi.

article. A total of 100 copies of each protein fragment pair were equilibrated at 2000 K with the p53 side-chain atoms reduced in atomic radius, bond lengths, and electrostatic and van der Waals forces to create molecular models of the p53–CHC complex. The equilibrated molecules underwent simulated annealing along with growing the p53 side chains to their original sizes and energies. After generating a probability density map using the 100 copies of the p53–CHC complex, the best-fit structure was derived by simulated annealing to the probability density map of the complex. Resulting structural analyses by MCSA-PCR revealed that residues Leu43, Leu45, Ile50, and Trp53 of p53 were varied in the hydrophobic cavity of CHC and that Trp53 of p53 was stacked near Phe1327 of CHC through these aromatic rings (Fig. 3a). Notably, a side chain of Asn1288 of CHC appeared to contact a side chain of Gln38 of p53 (Fig. 3b); in contrast, Asn1288 of CHC is unlikely to be a contact site with CLC. In fact, a substitution of Asn1288 to Ala in CHC diminishes its ability to bind to p53 without any effect on CHC–CLC interaction, though CLC binds to a similar region in CHC with p53 (see below). Interestingly, this Asn1288 in CHC is a conserved residue in multicellular organisms from mammals to flies, but this residue is not present in unicellular organisms such as yeasts and fungi (Fig. 3c).

An Asn1288 residue in CHC is important for binding to p53

In order to examine the requirement of Asn1288 residue in CHC for binding to p53, we substituted Asn1288 to Ala of CHC bearing residues from 833 to 1406 to generate a CHC833–1406-N1288A mutant. The region from residues 833 to 1406 of CHC is defined as the interaction domain with p53 to trans-

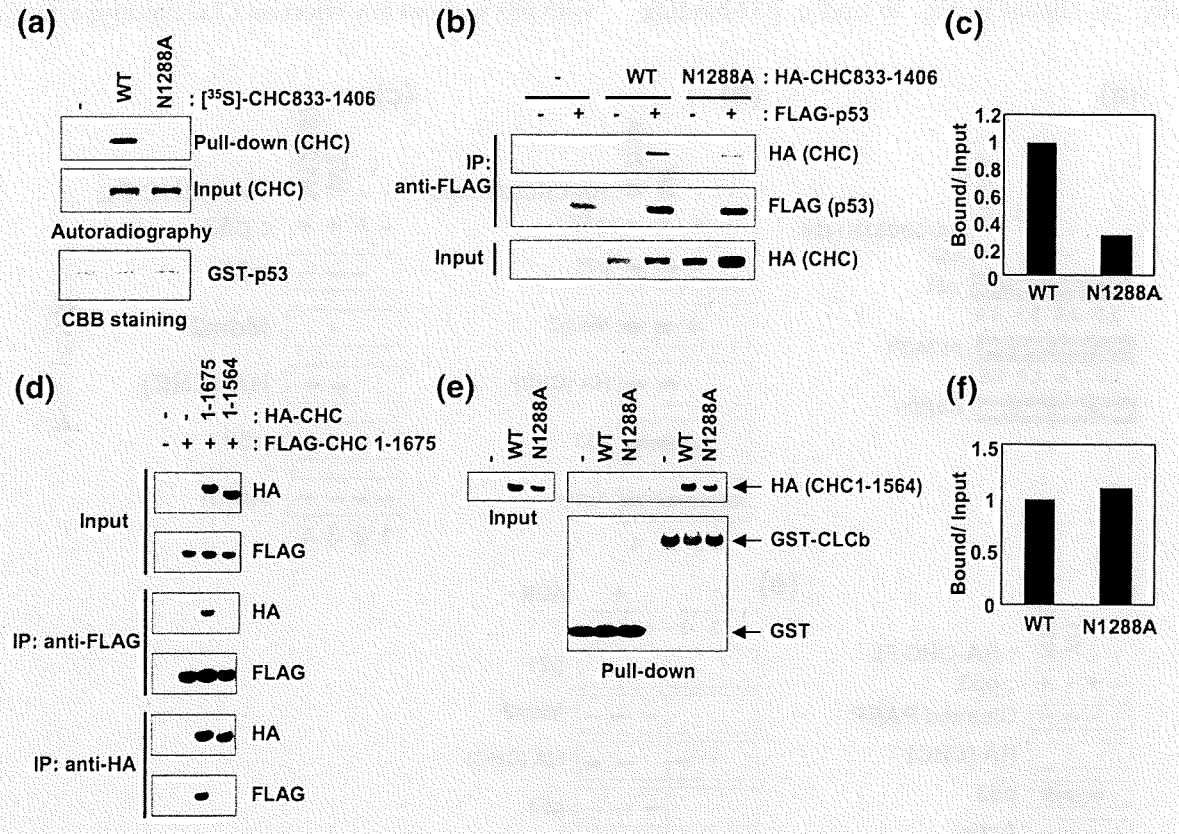

Fig. 4. Substitution of Asn1288 to Ala in CHC diminishes its ability to interact with p53. (a) *In vitro* binding assay for p53–CHC interaction. ^{35}S-labeled CHC833–1406 proteins (wild type and N1288A) were synthesized and used for *in vitro* binding assay as above. (b) Binding assay for p53–CHC interaction in cells. H1299 cells were transfected with FLAG-p53 and each HA-CHC833–1406 construct. FLAG-p53 was immunoprecipitated by anti-FLAG antibody, and eluates were loaded on a 5–20% gradient SDS-PAGE gel, followed by immunoblotting with anti-HA or anti-FLAG antibodies. (c) The graph represents the fold binding relative to input signal as quantified by Image J densitometry. (d) CHC lacking trimerization domain (CHC1–1564) does not interact with full-length CHC (CHC1–1675). H1299 cells were transfected with each HA-CHC construct and FLAG-CHC1–1675. Samples immunoprecipitated by either anti-HA or anti-FLAG antibody were separated by SDS-PAGE, followed by immunoblotting with indicated antibodies. The samples were run in the same gel and then combined side by side. (e) CHC1–1564 harboring N1288A interacts with CLC equivalent to wild-type CHC. HA-CHC1–1564 proteins (wild type and N1288A) were synthesized by an *in vitro* transcription-coupled translation system using rabbit reticulocyte lysates. Lysates containing HA-CHC protein were mixed with GST or GST-CLC immobilized on glutathione-Sepharose 4B beads for binding assay, separated by SDS-PAGE, and followed by immunoblotting with indicated antibodies. (f) The graph represents the fold binding relative to input signal as quantified by Image J densitometry.

activate it and has neither the ability to form trimerization nor the ability to bind to CLC.[21] The trimerization domain of CHC interacts with endogenous CHC, and the CLC-binding domain interferes with the binding of p53 to CHC.[21] Thus, these domains may be obstructed to assess the effect of a point mutation of CHC on the interaction with p53 and we used a CHC deletion mutant lacking trimerization and CLC-binding domains for an *in vitro* p53-binding assay. A GST pull-down assay showed that an N1288A mutation in the CHC833–1406 protein diminished its ability to interact with p53, although wild-type CHC was able to bind p53 (Fig. 4a). Furthermore, we tested whether N1288A of CHC causes decreased p53-binding affinity in cells. A FLAG-tagged p53 construct was cotransfected with empty vector, HA-tagged CHC833–1406-WT, or HA-tagged CHC-833–1406-N1288A in cells, and cell lysates were immunoprecipitated with anti-FLAG antibody followed by immunoblotting with anti-HA antibody. As shown in Fig. 4b and c, p53-binding affinity of mutated CHC was reduced up to 30% compared with wild-type CHC, indicating that this N1288 residue in CHC protein is crucial for interaction between CHC and p53. We have previously found that CLC binds to CHC at the C-terminal region proximal to p53-binding sites and inhibits the interaction of p53 with CHC. To assess whether this substitution affects CLC-binding activity, we constructed an N1288A mutant of CHC lacking residues from 1565 to 1675 (CHC1–1564), which does not possess a trimerization domain that interacts with full-length CHC (Fig. 4d), and performed a GST pull-down assay using GST fused to CLCb (GST-CLCb). HA-tagged CHC1–1564 proteins produced by an *in vitro* transcription/translation system using rabbit reticulocyte lysates were used for this assay. Interestingly, the N1288A mutation had little effect on the ability to interact with CLC (Fig. 4e and f). Taken together, these results indicate that an N1288A mutation of CHC specifically influences interaction with p53 without any effect on CLC-binding activity.

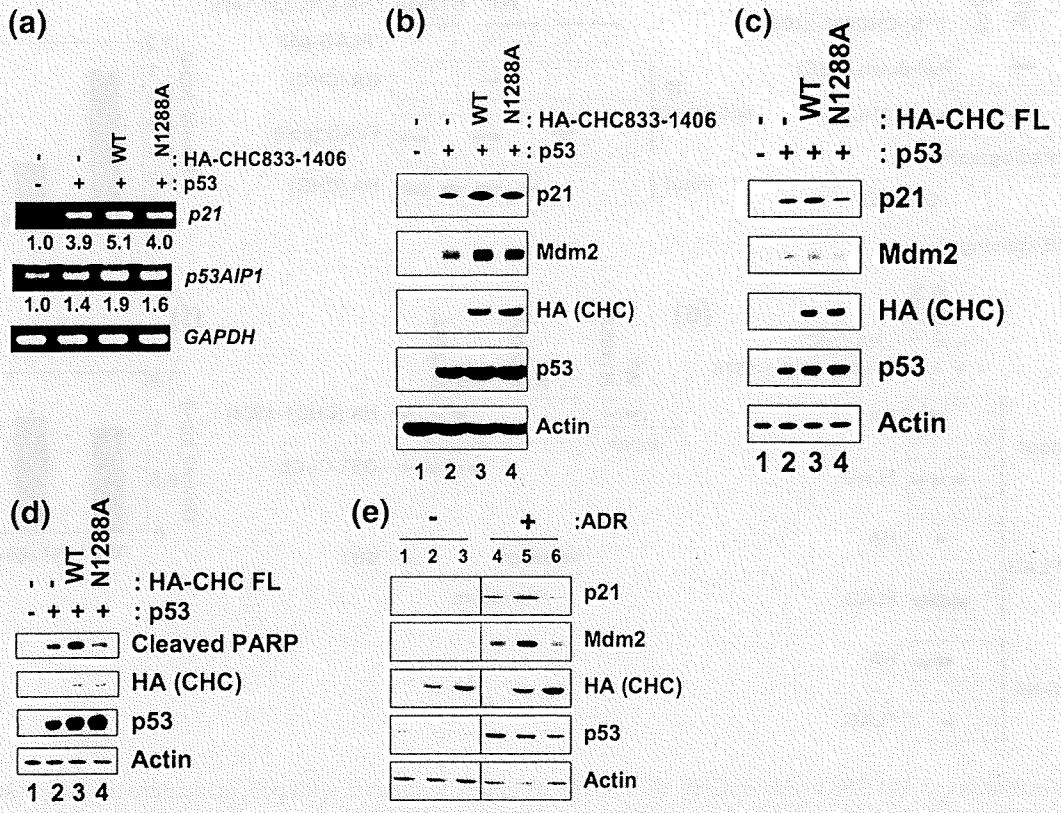

Fig. 5. An N1288A mutation of CHC abolishes the ability to transactivate p53. (a) H1299 cells were transfected with p53 and each HA-CHC833–1406 construct. Expression levels of p53-target genes were analyzed by semiquantitative RT-PCR. The intensity of PCR products was quantified by Image J software. (b) H1299 cells were transfected as described in (a), and whole-cell lysates were analyzed by immunoblotting using the indicated antibodies. (c) Full-length CHC-N1288A acts as a dominant-negative mutant. H1299 cells were transfected with p53 and each HA-tagged full-length CHC construct, and whole-cell lysates were analyzed by immunoblotting using the indicated antibodies. (d) Full-length CHC-N1288A inhibits p53-mediated apoptosis. H1299 cells were transfected with p53 and each HA-tagged CHC construct, incubated for 24 h, and the cleaved PARP was detected by immunoblotting with anti-cleaved PARP antibody. (e) Full-length CHC-N1288A blocks the induction of p53-target genes activated by DNA damage. HT-1080 cells were transfected with an empty vector, wild-type CHC, or CHC-FL-N1288A construct, and stable transformants were obtained by G418 selection. These cells were treated without (lanes 1 to 3) or with (lanes 3 to 6) 0.5 μM adriamycin (ADR) for 6 h. Cell lysates from cells transfected with empty vector (lanes 1 and 4), wild-type CHC (lanes 2 and 5), or CHC-FL-N1288A (lanes 3 and 6) were subjected to immunoblotting with indicated antibodies.

CHC-N1288A mutant abolishes the ability to transactivate p53

Given that the N1288 residue in CHC is crucial for interaction with p53, we next examined the effect of an N1288A mutation of CHC on p53 transactivation. Reverse transcriptase–polymerase chain reaction (RT-PCR) analysis revealed that CHC833–1406-WT had the activity to enhance p53 transactivation, but CHC833–1406-N1288A failed to enhance the induction of p53-target genes such as p21 and p53AIP1 (Fig. 5a). In addition, we confirmed that CHC833–1406-N1288A abolished the ability to enhance the induction of p53-target genes by immunoblot analysis (Fig. 5b). To further confirm the effect of N1288A mutation on p53-mediated transcription, we used full-length CHC constructs with or without this mutation. Full-length wild-type CHC increased expression levels of both p21 and Mdm2 in a p53-dependent manner; in contrast, full-length CHC harboring an N1288A mutation (CHC-FL-N1288A) abrogated the ability to enhance p53 transactivation (Fig. 5c). Interestingly, CHC-FL-N1288A appears to behave as a dominant-negative mutant.

Expression of p53 in p53-null cells induces apoptosis accompanied with caspase-3/7 activation and the cleavage of poly-ADP ribose polymerase (PARP) known as a substrate of caspase-3/7.[13,21]

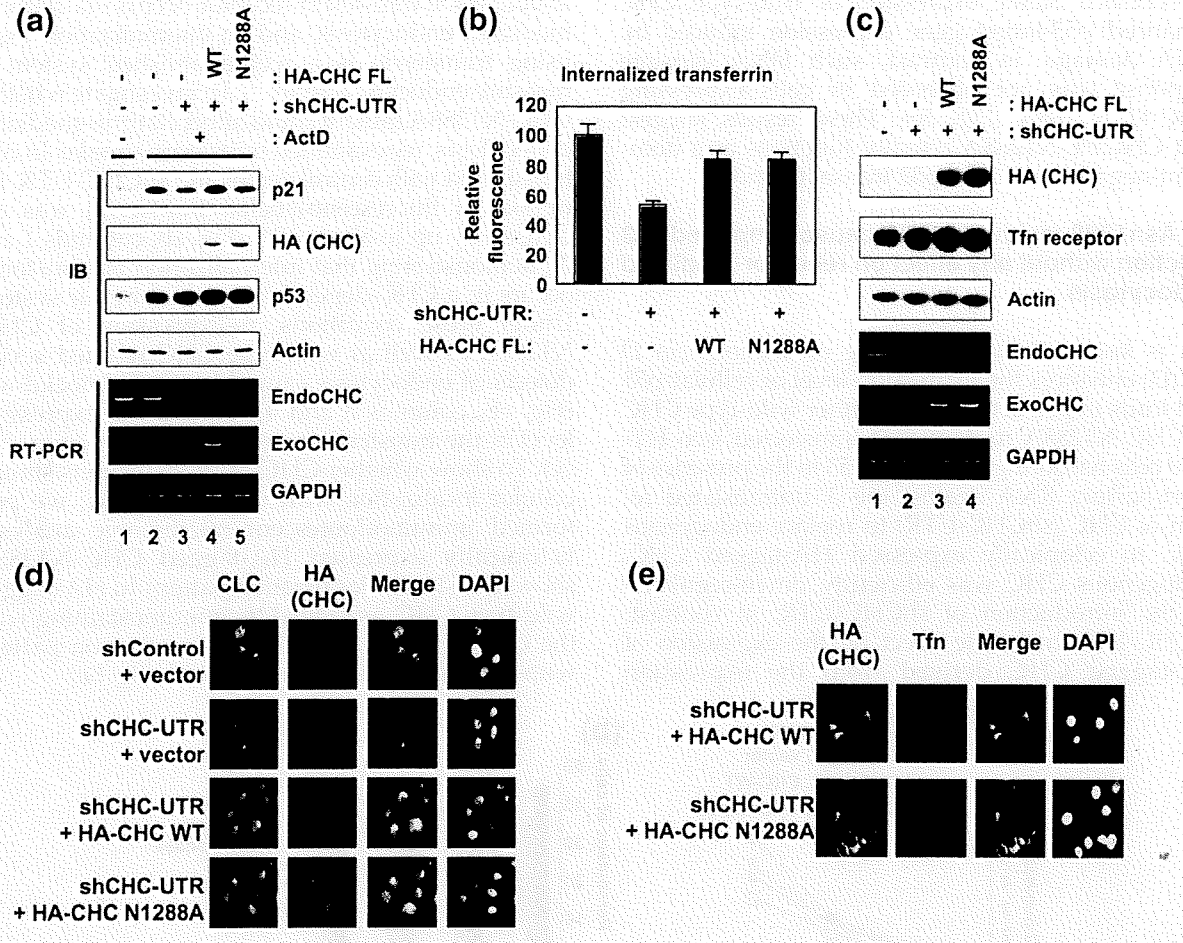

Fig. 6. An N1288A mutation in full-length CHC causes a severe defect in the regulation of p53-mediated transcription, but its CHC mutant preserves function for receptor-mediated endocytosis. (a) HT-1080 cells were transfected with shCHC-UTR and each HA-tagged full-length CHC construct, treated with 5 nM ActD for 6 h, and cell lysates were analyzed by immunoblotting using the indicated antibodies and by RT-PCR using primers specific for endogenous CHC (EndoCHC) and ectopically expressed CHC (ExoCHC). Actin and GAPDH were used as loading controls for immunoblotting and RT-PCR, respectively. (b) HeLa cells were transfected with indicated plasmids plus a green fluorescent protein expression plasmid. Three days after transfection, cells were incubated for 8 min at 37 °C in DMEM containing 20 μg/mL of AlexaFluor594-conjugated transferrin (AF594-transferrin) and 0.1% BSA. After the removal of cell-surface-bound AF594-transferrin, these cells were trypsinized and fixed with 4% paraformaldehyde. For measurement of AF594-transferrin uptake, green fluorescent protein-positive cells were quantified by flow cytometric analysis. (c) Proteins and total RNA in whole-cell lysates from cells used for (b) were analyzed by immunoblotting and RT-PCR, respectively. (d) A CHC-N1288A mutant co-localizes with CLC, similarly to wild-type CHC. HeLa cells were transfected with the indicated plasmids and immunostained with anti-HA (green) and anti-CLC (red) antibodies 72 h after transfection. (e) An N1288A mutation has little effect on the localization of transferrin. HeLa cells were transfected with the indicated plasmids, and the uptake of AF594-transferrin (red) was carried out as in (b). After the removal of cell-surface-bound AF594-transferrin, these cells were immunostained with anti-HA (green) antibody.

Therefore, we next addressed the effect of an N1288A mutation in full-length CHC on p53-mediated apoptosis. Caspase activation is an important event for apoptosis and it was monitored using the cleavage of PARP. Immunoblot analysis showed that co-expression of p53 and wild-type CHC increased cleavage of PARP compared with p53 alone (Fig. 5d), consistent with our previous data that CHC enhances p53-mediated apoptosis. In contrast, CHC-N1288A inhibited p53-induced PARP cleavage (Fig. 5d), suggesting that an N1288A mutation in CHC abolishes the ability to undergo apoptosis mediated by p53. To evaluate CHC-FL-N1288A works as a dominant-negative effect, we generated cells stably expressing CHC-FL-N1288A. Stable expression of wild-type CHC enhanced p53-target gene expression induced by DNA damage; in contrast, such DNA damage response was not observed in cells expressing CHC-FL-N1288A (Fig. 5e). These results suggest that CHC-FL-N1288A actually functions as a dominant-negative effect on p53 transactivation.

An Asn1288 residue in CHC causes impaired p53 function without any effect on receptor-mediated endocytosis

It is known that a low dose of actinomycin D (ActD) enhances the expression level of cellular p53 and leads to p53 activation.[27] Either wild-type CHC or CHC-N1288A mutant was transfected into HT-1080 cells harboring wild-type p53 in the presence of short-hairpin RNA against the 3′-untranslated region of CHC (shCHC-UTR) to replace endogenous CHC to ectopically expressed HA-tagged CHC. Endogenous CHC was efficiently down-regulated by the introduction of shCHC-UTR; in contrast, shCHC-UTR had little effect on the expression of HA-tagged CHC derived from the expression plasmid, as confirmed by RT-PCR using primers specific for endogenous and ectopically expressed CHC (Fig. 6a). Partial knockdown of CHC attenuates the induction of p21 in response to ActD (Fig. 6a, lanes 2 and 3), as shown in our previous report.[15] Re-expression of HA-tagged wild-type CHC in CHC-depleted cells recovered DNA damage response to up-regulate p21 expression (Fig. 6a, lanes 3 and 4), whereas swapping of endogenous CHC with HA-tagged CHC bearing a N1288A mutation did not rescue p21 induction (Fig. 6a, lane 5). Taken together, these results demonstrate that Asn1288 in CHC is crucial for interaction with p53 to promote sufficient induction of p53-mediated transcription.

It has been shown that ligand-induced internalization of the transferrin receptor occurs via clathrin-mediated endocytosis, and an internalization assay using transferrin is a well-established system to measure endocytic activity.[28] To investigate whether CHC-N1288A mutant could affect clathrin-mediated endocytosis, we examined transferrin uptake. In cells transfected with control vector and shCHC-UTR, the uptake of fluorescent-labeled transferrin was decreased by up to about 50% (Fig. 6b, columns 1 and 2), demonstrating that internalization of transferrin occurs in a CHC-dependent manner in our system. Under these conditions, re-expression of CHC-N1288A as well as wild-type CHC rescued severe defects of endocytosis caused by CHC knockdown (Fig. 6b, columns 3 and 4), though the expression level of the transferrin receptor was invariable (Fig. 6c). To show whether CHC-N1288A exhibits similar cellular localization with wild-type CHC, we performed immunofluorescent microscopic analysis. Ectopically expressed HA-tagged CHC-N1288A showed a similar localization pattern to HA-tagged wild-type CHC, as judged by immunostaining with the CLC (Fig. 6d) or by the co-localization pattern with fluorescent-labeled transferrin (Fig. 6e).

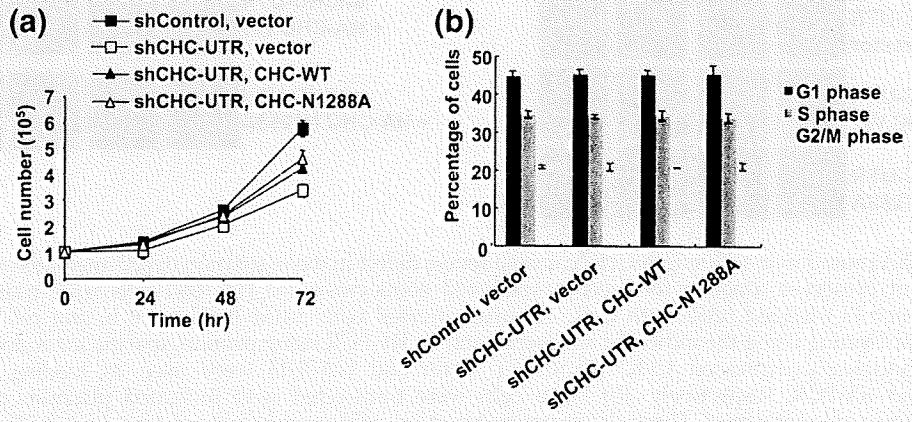

Fig. 7. An N1288A mutation in CHC has little or no effect on cell viability and cell-cycle progression. (a) A CHC-N1288A mutant has the ability to recover the proliferation of CHC-depleted cells as efficiently as that of wild-type CHC. Twenty-four hours after transfection with the indicated plasmids, these HT-1080 cells were collected and then plated in 60-mm culture dishes. Cell numbers were determined with a hemocytometer after the indicated times. Data represent the mean values from three independent experiments with error bars. (b) N1288A mutation did not impact on cell-cycle progression. HT-1080 cells were transfected as in (a), and these cells cultured for 72 h after transfection were subjected to flow cytometric analysis. DNA content was monitored by propidium iodide staining, and the percentages of the cells in G1, S, and G2/M phases were determined using ModFit LT software. Data represent the mean values from three independent experiments with error bars.

CHC is an essential gene for cell viability, and complete ablation of CHC expression leads to cell death.[29] Therefore, we next assessed whether an N1288A mutation in CHC influences cell viability. As shown in Fig. 7a, CHC-depleted cells expressing CHC-FL-N1288A exhibited no lethality, unlike CHC-depleted cells transfected with a control vector, and they showed a similar growth rate to CHC-depleted cells re-expressing wild-type CHC. We also confirmed that N1288A mutation did not influence mitosis as judged by flow cytometric analyses (Fig. 7b). Taken together, these data demonstrate that an N1288A mutation in CHC abolishes its abilities to interact with and to transactivate p53 without any effects on receptor-mediated endocytic activity and cell viability. Our findings provide a useful tool for understanding a role of CHC in p53-mediated transcription, distinct from receptor-mediated endocytosis.

Discussion

CHC has originally been identified as a cytosolic protein that functions in vesicle transport and endocytosis.[10–12] It has recently been shown that CHC is also involved in the maintenance of mitotic spindle as its additional function.[19] We have previously found an alternative function of CHC that promotes p53-mediated transcription in nuclei and that the enhancement of p53 transactivation by CHC required the interaction of the N-terminal transactivation domain of p53 with CHC.[13] Although the trimerization domain of CHC is important for functions in vesicle transport, endocytosis, and mitosis,[23] it is indispensable for p53-mediated transcription. These findings implicate that nuclear CHC works via a distinct mechanism from cytosolic CHC.[21] In addition, our recent studies showed that partial knockdown of CHC attenuated p53 transactivation, but we could not rule out a possibility that CHC knockdown may cause undetectable side effects on CHC-mediated endocytosis essential for cell survival and proliferation.[29]

We have previously noticed that the N-terminal region of p53 around Ser46 has a considerable similarity with the CHC-binding region of CLC and an essential Trp residue for binding to CHC in CLC is conserved in p53.[13] Conceivably, CLC competes with p53 through this homologous region in binding to CHC, and both p53 and CLC associate with CHC in a mutually exclusive manner.[13] In this study, we generated various p53 point mutants and determined the detailed residues responsible for binding to CHC. *In vitro* binding assay revealed that several hydrophobic residues, including Trp53 in p53, are required for interaction with CHC. Furthermore, mutations of these hydrophobic residues in p53 strikingly impaired the transcriptional activity compared with wild-type p53. Thus, these results indicate that conserved residues between p53 and CLC are required for both CHC binding and p53 transactivation and that the ability of p53 to interact with CHC correlates with p53 transcriptional activity.

We generated more than 20 constructs for CHC fragments containing the p53-binding region to determine the tertiary structure of the p53–CHC complex, but these CHC fragments had poor solubility and it was difficult to obtain the structural information of the p53–CHC complex (data not shown). Therefore, based on tertiary structures of the N-terminus of p53 and CHC already determined by NMR and X-ray crystallography in combination with information obtained from our present p53–CHC-binding studies, a preliminary molecular model of the p53–CHC interaction was constructed, although it remains to be determined whether CHC induces α-helical conformation of the N-terminus of p53, which is observed when forming a complex with RPA70 (replication protein A70) or with p62, a subunit of TFIIH.[26,30] This molecular modeling predicted that Asn1288 in CHC might be important for p53–CHC interaction because this residue is close to a side chain of Glu38 of p53. As expected, a substitution of the Asn1288 to Ala diminished the ability to bind p53 and to enhance p53 transactivation. We also found that an Asn-to-Ala-substituted full-length CHC (CHC-FL-N1288A) appears to behave as a dominant-negative mutant unlike CHC833–1406-N1288A. These findings suggest that the region depleted in CHC competes with endogenous CHC to trap some p53 co-activators, such as p300/CBP, because CHC interacts with p300/CBP to stabilize the association with p53.[13] On the other hand, CHC-FL-N1288A did not affect the ability to bind to CLC, transferrin uptake, and the cellular localization of CLC, and growth arrest induced by endogenous CHC knockdown was reverted by the expression of CHC-FL-N1288A as well as the introduction of wild-type CHC. In respect to the impact of partial CHC knockdown on G2/M phase, no alteration was observed, at least under our conditions. Taken together, these results suggest that this mutant influences the p53 pathway without any effect on CHC-mediated endocytosis essential for cell survival.

CHC is an essential gene for cell viability, and complete ablation of CHC expression leads to cell death accompanied by the activation of Akt-mediated and mitogen-activated protein kinase-mediated pathways.[29] In contrast, point mutations of some essential genes have often little effect on cell viability. For example, cytochrome *c* plays important roles in electron transport and apoptosis, but cytochrome *c* bearing a K72A point mutation is defective in apoptotic regulation without affecting the function of electron transport essential for cell viability.[31] Therefore, such a CHC point mutant will help to dissect physiological functions of CHC in the regulation of the p53 pathway.

Interestingly, the alignment of primary structures between species revealed that this Asn1288 in CHC was conserved in multicellular organisms from mammals to flies, but this amino acid residue was not present in unicellular organisms such as yeasts

and fungi (Fig. 2c). In multicellular organisms, the p53–CHC system may have evolved to acquire a complicated regulatory function in response to various cellular damages to maintain multicellular homeostasis.

In summary, we predicted a preliminary binding interface between p53 and CHC and found that an Asn1288 in CHC was critical for interaction with p53 but not with CLC. Using such a CHC mutant preserving endocytic function, specific disruption of the function of CHC as a p53 regulator in mice will clarify physiological functions of CHC in the regulation of the p53 pathway. In addition, there are no reports of cancer-associated mutations in the CHC gene so far and it is interesting to search for mutations in the p53-binding region of CHC, in particular the region around Asn1288, in tumor samples from patients. Further investigations will be needed to elucidate the role of CHC in tumorigenesis.

Materials and Methods

Cell culture and transfection

Human lung carcinoma H1299 cells were grown in RPMI 1640 medium supplemented with 10% fetal bovine serum and penicillin/streptomycin. Human fibrosarcoma HT-1080 cells and human cervical carcinoma HeLa cells were grown in Dulbecco's modified Eagle's medium (DMEM) supplemented with 10% fetal bovine serum and penicillin/streptomycin at 37 °C in a 5% CO_2 atmosphere. For transfection, cells were plated at 80–90% confluency the day before transfection and transfected with Lipofectamine 2000 reagent (Invitrogen) according to the manufacturer's protocol.

Antibodies

Horseradish peroxidase (HRP)-conjugated anti-p53 (DO-1), HRP-conjugated anti-Actin (C-2), anti-CLC (CON.1), and anti-GST (B-14) antibodies were purchased from Santa Cruz Biotechnology Inc. Anti-p21 (SX118) and anti-CHC (clone 23) antibodies were from BD Pharmingen. Anti-HA (6E2), anti-HA (C29F4), and anti-cleaved PARP antibodies were obtained from Cell Signaling Technology. Anti-Mdm2 (IF2), anti-FLAG (M2), and anti-transferrin receptor antibodies were purchased from Calbiochem, SIGMA, and Zymed, respectively. HRP-conjugated secondary antibodies were obtained from GE Healthcare.

Immunoprecipitation and immunoblot analysis

H1299 cells were extracted with lysis buffer [50 mM Tris at pH 7.2, 250 mM NaCl, 2 mM $MgCl_2$, 0.1 mM ethylenediaminetetraacetic acid, 0.1 mM ethylene glycol bis(β-aminoethyl ether)*N*,*N*′-tetraacetic acid, 0.1% Nonidet P-40, 0.5 mM DTT, 10 μg/mL antipain, 10 μg/mL pepstatin A, 10 μg/mL chymostatin, 10 μg/mL leupeptin, 10 μg/mL E-64, 10 μg/mL PMSF, 1 mM Na_3VO_4, and 5 mM NaF] for 20 min on ice, and the lysates were cleared by centrifugation at 20,000*g* for 20 min. For immunoprecipitation, the supernatants were incubated with 10 μL of anti-FLAG M2 agarose beads (SIGMA) for 3 h at 4 °C and washed three times with lysis buffer. The bound proteins were eluted with FLAG peptide (SIGMA) at 4 °C for 30 min, separated by SDS-PAGE (Biocraft), followed by transfer to polyvinylidene fluoride membranes (Millipore). The membranes were blocked with 5% skim milk in TBST buffer (20 mM Tris at pH 7.6, 137 mM NaCl, and 0.1% Tween 20) and incubated with the first antibody. The blots were washed three times with TBST buffer, incubated with the secondary antibody conjugated to HRP, and then washed five times with TBST buffer. The bands of interest were visualized by ECL chemiluminescence (GE Healthcare).

Reporter assay

A reporter assay was performed as described previously.[13] In brief, H1299 cells plated on 24-well plates were transfected with 1 ng of p53-SN3 and 150 ng of the indicated reporter vectors in combination with 10 ng of phRG-TK encoding Renilla luciferase as an internal control using Lipofectamine 2000. Twenty-four hours after transfection, cells were harvested and luciferase activity was quantified by a dual luciferase assay system (Promega) according to the manufacturer's instructions.

RT-PCR analysis

RT-PCR analysis was performed as described previously.[13] Briefly, total RNA was isolated using an RNeasy Mini kit (QIAGEN) and reverse-transcribed with the SuperScript First-Strand Synthesis System for RT-PCR kit (Invitrogen). Reverse-transcribed products were used in the PCR reactions. PCR programs and primer sequences were described previously.[13] PCR products were analyzed using 2% agarose gel electrophoresis and ethidium bromide staining. The amplified DNA fragments were quantified by Image J version 1.41 densitometry.

GST pull-down assay

To analyze the interaction between p53 and CHC, we performed a GST pull-down assay as described previously.[13] In brief, bacterial lysates containing p53 derivatives fused to GST were incubated with glutathione-Sepharose 4B beads (GE Healthcare) and washed extensively with binding buffer [50 mM Tris at pH 7.2, 250 mM NaCl, 2 mM $MgCl_2$, 0.1 mM ethylenediaminetetraacetic acid, 0.1 mM ethylene glycol bis(β-aminoethyl ether)*N*,*N*′-tetraacetic acid, 0.1% Tween 20, 0.5 mM DTT, 10 μg/mL antipain, 10 μg/mL pepstatin A, 10 μg/mL chymostatin, 10 μg/mL leupeptin, 10 μg/mL E-64, 10 μg/mL PMSF, 1 mM Na_3VO_4, and 5 mM NaF]. ^{35}S-labeled CHC derivatives were synthesized using an *in vitro* transcription/translation-coupled reticulocyte lysate system (Promega) and incubated with the above beads immobilized with GST-p53 derivatives at 4 °C for 2 h. After washing with 1 mL of binding buffer, bound proteins were eluted by boiling in SDS sample buffer for 5 min, subjected to SDS-PAGE, and analyzed by autoradiography.

RNA interference

For the expression of short-hairpin RNA against the 3′-UTR of CHC mRNA, synthetic oligo DNAs, 5′-GATCCCCAGAGCACCATGATTCCAATTTCAAGAGATTGGAATCATGGTGCTCTTTTTTGGAAA-3′ and 5′-

AGCTTTTCCAAAAAGAGCACCATGATTC-CAATTCTCTTGAAATTGGAATCATGGTGCTCTGGG-3′, were annealed and inserted into the pSUPER vector (shCHC-UTR) and transfected in HT-1080 and HeLa cells, as described above. To confirm the suppression of endogenous CHC expression, we used synthetic primers: CHC-S (5′-CCAGGCACCTTTTGGTTATG-3′) and CHC-AS (5′-CTTTCATGCCTCCCTAATGC-3′) for the detection of endogenous CHC and CHC-S and pcDNA3.1-AS (5′-ACTCAGACAATGCGATGCAA-3′) or pCAGGS-AS (5′-CCCATATGTCCTTCCGAGTG-3′) for ectopically expressed CHC.

Endocytosis assay, cell proliferation, and cell-cycle analyses

To analyze the effect of CHC mutants on endocytic activity, we transfected HeLa cells with 1 μg of shCHC-UTR plus 2 μg of pCAGGS-CHC vectors in combination with 50 ng of pmaxGFP vector (Amaxa), as a transfection marker. Three days after transfection, cells were incubated in DMEM containing 0.1% bovine serum albumin (BSA) for 3 h, followed by treatment with 20 μg/mL Alexafluor594-conjugated transferrin (AF594-transferrin, Molecular Probes) for 8 min at 37 °C. Cells were rapidly chilled by extensive washing with ice-cold PBS, and then AF594-transferrin bound on the cell surface was removed by washing with ice-cold acid-washing buffer containing 0.2 M acetic acid (pH 4.5) and 0.5 M NaCl. These cells were trypsinized, fixed with 4% paraformaldehyde in PBS for 20 min at room temperature, and resuspended in 0.1% BSA in PBS. Relative fluorescence was quantified by flow cytometric analysis (Becton Dickinson) for internalized AF594-transferrin.

HT-1080 cells transfected with the indicated expression vectors were collected 24 h after transfection and then plated in 60-mm culture dishes to analyze the effect of CHC-N1288A on cell proliferation. Cell numbers were determined with a hemocytometer after the indicated times.

For cell-cycle analysis, HT-1080 cells were transfected with the indicated expression vectors for 72 h and then fixed in 70% ethanol at −20 °C for several hours. Cells were centrifuged at 600*g* for 5 min and resuspended in PBS containing 0.1 mg/mL RNase A (QIAGEN). Samples were incubated at 37 °C for 30 min, and propidium iodide (SIGMA) was added to make a final concentration of 25 μg/mL. Samples were analyzed by a FACSCalibur flow cytometer using CellQuest software (BD Biosciences), and the percentages of the cells in G1, S, and G2/M phases of the cell cycle were determined using ModFit LT software.

Immunofluorescence

HeLa cells transfected with shCHC-UTR and pCAGGS-CHC were plated on an 8-well Lab-Tek II Chamber Slide (Nalge Nunc), fixed in 4% paraformaldehyde in PBS for 20 min, permeabilized with 0.1% Triton X-100 in PBS for 5 min, and blocked with PBS containing 3% BSA. The cells were sequentially incubated with anti-HA (C29F4) and/or anti-CLC antibodies and with AlexaFluor-conjugated secondary antibody (Molecular Probes) and mounted with a Vectashield reagent with 4′,6-diamidino-2-phenylindole (Vector Laboratories). Immunofluorescence was performed using a Nikon ECLIPSE E1000 fluorescence microscope (Nikon Corporation).

Structural modeling of p53–CHC interaction

To generate an initial model of the side chains in the p53–CHC interface, we used a model of CLC and CHC interface[25] as a template. A partial structure of p53 (residues 33–56) taken from the crystallographic structure of p53/RPA70 complex[26] was then overlaid manually to the backbone atoms of the corresponding region of CLC. The detailed backbone orientation was further established by rotational search and energy minimization. This docked model served as the starting point for MCSA-PCR. During the MCSA-PCR, all side-chain atoms of p53 were free to move, and backbone C^{α} atoms in the second α-helix of p53 (residue 46–56) were weakly restrained (5 kcal mol^{-1} A^{-2}) to the corresponding residues of CLC (residue 97–107). For the first α-helix of p53 (residue 35–40), nuclear Overhauser effect distance restraints (2.86± 1 Å) were weakly assigned between the p53 backbone carbonyls and amides in order to promote the helicity of p53, but allowing the deviation from the original helix structure. Then, an ensemble of 100 possible structures was produced by growing side-chain atoms with simulated annealing methods. This was refined to a single best-fit structure through MCSA-pseudo-crystallographic refinement.[24] The final structure was refined against a pseudo-density map generated from the ensemble using standard crystallographic techniques. All calculations were carried out in gas phase with X-PLOR, using the OPLS (optimized potentials for liquid simulations) force field for polar hydrogens.[32]

Acknowledgements

We thank B. Vogelstein for WWP-Luc and the members of Taya and Yokota lab for helpful discussions. This work was partly supported by SORST, Japan Science and Technology Corporation (to Y.T.), MEXT, KAKENHI (17013088) (to Y.T. and M.E.), a Grant-in-Aid from the Ministry of Health, Labor and Welfare for the 3rd Term Comprehensive 10-year Strategy for Cancer Control (to Y.T. and M. E.), and a grant from the Takeda Science Foundation (to M.E.).

References

1. Toledo, F. & Wahl, G. M. (2006). Regulating the p53 pathway: in vitro hypotheses, in vivo veritas. *Nat. Rev. Cancer*, **6**, 909–923.
2. Bourdon, J. C., Laurenzi, V. D., Melino, G. & Lane, D. (2003). p53: 25 years of research and more questions to answer. *Cell Death Differ.* **10**, 397–399.
3. Vousden, K. H. & Lu, X. (2002). Live or let die: the cell's response to p53. *Nat. Rev. Cancer*, **2**, 594–604.
4. Vogelstein, B., Lane, D. & Levine, A. J. (2000). Surfing the p53 network. *Nature*, **408**, 307–310.
5. Ljungman, M. (2000). Dial 9-1-1 for p53: mechanisms of p53 activation by cellular stress. *Neoplasia*, **2**, 208–225.
6. Prives, C. & Hall, P. A. (1999). The p53 pathway. *J. Pathol.* **187**, 112–126.
7. Levine, A. J. (1997). p53, the cellular gatekeeper for growth and division. *Cell*, **88**, 323–331.

8. Hollstein, M., Sidransky, D., Vogelstein, B. & Harris, C. C. (1991). p53 mutations in human cancers. *Science*, **253**, 49–53.
9. Samuels-Lev, Y., O'Connor, D. J., Bergamaschi, D., Trigiante, G., Hsieh, J. K., Zhong, S. *et al.* (2001). ASPP proteins specifically stimulate the apoptotic function of p53. *Mol. Cell*, **8**, 781–794.
10. Willingham, M. C. & Pastan, I. (1984). Endocytosis and exocytosis: current concepts of vesicle traffic in animal cells. *Int. Rev. Cytol.* **92**, 51–92.
11. Takei, K. & Haucke, V. (2001). Clathrin-mediated endocytosis: membrane factors pull the trigger. *Trends Cell Biol.* **11**, 385–391.
12. Mellman, I. (1996). Endocytosis and molecular sorting. *Annu. Rev. Cell Dev. Biol.* **12**, 575–625.
13. Enari, M., Ohmori, K., Kitabayashi, I. & Taya, Y. (2006). Requirement of clathrin heavy chain for p53-mediated transcription. *Genes Dev.* **20**, 1087–1099.
14. Ishii, K., Hirano, Y., Araki, N., Oda, T., Kumeta, M., Takeyasu, K. *et al.* (2008). Nuclear matrix contains novel WD-repeat and disordered-region-rich proteins. *FEBS Lett.* **582**, 3515–3519.
15. Jasavala, R., Martinez, H., Thumar, J., Andaya, A., Gingras, A. C., Eng, J. K. *et al.* (2007). Identification of putative androgen receptor interaction protein modules: cytoskeleton and endosomes modulate androgen receptor signaling in prostate cancer cells. *Mol. Cell. Proteomics*, **6**, 252–271.
16. Endo, Y., Sugiyama, A., Li, S. A., Ohmori, K., Ohata, H., Yoshida, Y. *et al.* (2008). Regulation of clathrin-mediated endocytosis by p53. *Genes Cells*, **13**, 375–386.
17. Kirchhausen, T. (2000). Clathrin. *Annu. Rev. Biochem.* **69**, 699–727.
18. McPherson, P. S., Kay, B. K. & Hussain, N. K. (2001). Signaling on the endocytic pathway. *Traffic*, **2**, 375–384.
19. Royle, S. J., Bright, N. A. & Lagnado, L. (2005). Clathrin is required for the function of the mitotic spindle. *Nature*, **434**, 1152–1157.
20. Wakeham, D. E., Chen, C. Y., Greene, B., Hwang, P. K. & Brodsky, F. M. (2003). Clathrin self-assembly involves coordinated weak interactions favorable for cellular regulation. *EMBO J.* **22**, 4980–4990.
21. Ohmori, K., Endo, Y., Yoshida, Y., Ohata, H., Taya, Y. & Enari, M. (2008). Monomeric but not trimeric clathrin heavy chain regulates p53-mediated transcription. *Oncogene*, **27**, 2215–2227.
22. Huang, K. M., Gullberg, L., Nelson, K. K., Stefan, C. J., Blumer, K. & Lemmon, S. K. (1997). Novel functions of clathrin light chains: clathrin heavy chain trimerization is defective in light chain-deficient yeast. *J. Cell. Sci.* **110**, 899–910.
23. Royle, S. J. & Lagnado, L. (2006). Trimerisation is important for the function of clathrin at the mitotic spindle. *J. Cell. Sci.* **119**, 4071–4078.
24. Ota, N. & Agard, D. A. (2001). Binding mode prediction for a flexible ligand in a flexible pocket using multi-conformation simulated annealing pseudo crystallographic refinement. *J. Mol. Biol.* **314**, 607–617.
25. Chen, C. Y., Reese, M. L., Hwang, P. K., Ota, N., Agard, D. & Brodsky, F. M. (2002). Clathrin light and heavy chain interface: alpha-helix binding superhelix loops via critical tryptophans. *EMBO J.* **21**, 6072–6082.
26. Bochkareva, E., Kaustov, L., Ayed, A., Yi, G. S., Lu, Y., Pineda-Lucena, A. *et al.* (2005). Single-stranded DNA mimicry in the p53 transactivation domain interaction with replication protein A. *Proc. Natl Acad. Sci. USA*, **102**, 15412–15417.
27. Ashcroft, M., Taya, Y. & Vousden, K. H. (2000). Stress signals utilize multiple pathways to stabilize p53. *Mol. Cell. Biol.* **20**, 3224–3233.
28. Dautry-Varsat, A. (1986). Receptor-mediated endocytosis: the intracellular journey of transferrin and its receptor. *Biochimie*, **68**, 375–381.
29. Wettey, F. R., Hawkins, S. F., Stewart, A., Luzio, J. P., Howard, J. C. & Jackson, A. P. (2002). Controlled elimination of clathrin heavy-chain expression in DT40 lymphocytes. *Science*, **297**, 1521–1525.
30. Di Lello, P., Jenkins, L. M., Jones, T. N., Nguyen, B. D., Hara, T., Yamaguchi, H. *et al.* (2006). Structure of the Tfb1/p53 complex: insights into the interaction between the p62/Tfb1 subunit of TFIIH and the activation domain of p53. *Mol. Cell*, **22**, 731–740.
31. Hao, Z., Duncan, G. S., Chang, C. C., Elia, A., Fang, M., Wakeham, A. *et al.* (2005). Specific ablation of the apoptotic functions of cytochrome *c* reveals a differential requirement for cytochrome *c* and Apaf-1 in apoptosis. *Cell*, **121**, 579–591.
32. Jorgensen, W. L. & Tirado-Rives, J. (1988). The OPLS potential functions for proteins. Energy minimizations for crystals of cyclic peptides and crambin. *J. Am. Chem. Soc.* **110**, 1657–1666.

Cancer Science
The official journal of the Japanese Cancer Association
JCA

Prevalence of Human Papillomavirus 16/18/33 Infection and p53 Mutation in Lung Adenocarcinoma

Journal:	*Cancer Science*
Manuscript ID:	CAS-OA-0268-2010.R1
Manuscript Categories:	Original Article
Date Submitted by the Author:	28-Apr-2010
Complete List of Authors:	Iwakawa, Reika; National cancer center Research Institute, Biology Division Kohno, Takashi; National cancer center Research Institute, Biology Division Enari, Masato; National cancer center Research Institute, Biology Division Kiyono, Tohru; National cancer center Research Institute, Virology Division Yokota, Jun; National cancer center Research Institute, Biology Division
Keyword:	(7-1) Genomic analysis < (7) Cancer genome/genetics, (3-2) HPV < (3) Virus, infection and cancer, (14-3) Respiratory organ < (14) Characteristics and pathology of human cancer

Prevalence of Human Papillomavirus 16/18/33 Infection and p53 Mutation in Lung Adenocarcinoma

Reika Iwakawa[1], Takashi Kohno[1], Masato Enari[1], Tohru Kiyono[2], and Jun Yokota[1,3]

[1]Biology Division and [2]Virology Division, National Cancer Center Research Institute, Tokyo, Japan.

[3]To whom correspondence should be addressed

Postal address: 5-1-1, Tsukiji, Chuo-ku, Tokyo, 104-0045

E-mail: jyokota@ncc.go.jp

Fax: 03-3542-0807

Tel: 03-3547-5272

3991 words

2 tables / 1 figure

3 supporting tables